https://doi.org/10.5194/npg-2021-34
Preprint. Discussion started: 5 November 2021

Nonlinear Processes in Geophysics
Discussions
Open Access
EGU

Lévy-noise versus Gaussian-noise-induced Transitions in the Ghil-Sellers Energy Balance Model

Valerio Lucarini[1,2], Larissa Serdukova[1,2], and Georgios Margazoglou[1,2]

[1]Department of Mathematics and Statistics, University of Reading, Reading, UK.
[2]Centre for the Mathematics of Planet Earth, University of Reading, Reading, UK.

Correspondence: Valerio Lucarini (v.lucarini@reading.ac.uk)

Abstract. We study the impact of applying stochastic forcing to the Ghil-Sellers energy balance climate model in the form of a fluctuating solar irradiance. Through numerical simulations, we explore the noise-induced transitions between the competing warm and snowball climate states. We consider multiplicative stochastic forcing driven by Gaussian and α-stable Lévy - $\alpha \in (0,2)$ - noise laws, and examine the statistics of transition times and most probable transition paths. While the Gaussian noise case - used here as a reference - has been extensively studied in a plethora of studies on metastable systems, much less is known about the Lévy case, both in terms of mathematical theory and heuristics, especially in the case of high- and infinite-dimensional systems. In the weak noise limit, the expected residence time in each metastable state scales in a fundamentally different way in the Gaussian vs. Lévy noise case with respect to the intensity of the noise. In the former case, the classical Kramers-like exponential law is recovered. In the latter case, power laws are found, with the exponent equal to $-\alpha$, in apparent agreement with rigorous results obtained for additive noise in a related - yet different - reaction-diffusion equation as well as in simpler models. The transition paths are studied in a projection of the state space and remarkable differences are observed between the two different types of noise. The snowball-to-warm and the warm-to-snowball most probable transition path cross at the single unstable edge state on the basin boundary. In the case of Lévy noise, the most probable transition paths in the two directions are wholly separated, as transitions apparently take place via the closest basin boundary region to the outgoing attractor.

1 Introduction

1.1 Multistability of the Earth's Climate

The climate system comprises five interacting subdomains: the atmosphere, the hydrosphere (water in liquid form), the upper layer of the lithosphere, the cryosphere (water in solid form), and the biosphere (ecosystems and living organisms). The climate is driven by the inhomogeneous absorption of incoming solar radiation, which sets up nonequilibrium conditions. The system reaches an approximate steady state where macroscopic fluxes of energy, momentum, and mass are present throughtout its domain, and entropy is continuously generated and expelled into the outer space. The climate features variability on a vast range of spatial and temporal scales as a result of the interplay of forcing, dissipation, feedbacks, mixing, transport, chemical

https://doi.org/10.5194/npg-2021-34
Preprint. Discussion started: 5 November 2021


Nonlinear Processes in Geophysics
Discussions
Open Access
EGU

reactions, phase changes, and exchange processes between the subdomains; see Peixoto and Oort (1992) Lucarini et al. (2014a), Ghil (2015), and Ghil and Lucarini (2020).

In the late 1960s Budyko and Sellers independently proposed that in the current astronomical and astrophysical configuration the Earth could support two distinct climate states, the present day Warm (W), and a competing one characterised by global glaciation, which is the Snowball (SB) state. Their analysis was performed using one-dimensional energy balance models (EBM)s, which, despite their simplicity, were able to capture the essential physical mechanism in action, i.e. the interplay between two feedbacks associated with the energy exchange among the Earth, the Sun, and the space. The Boltzmann feedback is associated with the fact that warmer bodies emit more radiation, and is a negative, stabilizing one. Instead, the instability of the system is due to the presence of the so-called ice-albedo feedback: an increase in the ice-covered fraction of the surface leads to further temperature reduction of the planet because ice reflects efficiently the incoming solar radiation. These mechanisms are active at all spatial scales, including the planetary one; see Budyko (1969) and Sellers (1969). Such pioneering investigations of the multistability of the Earth's climate were later extended by Ghil (1976) and Ghil and Childress (1987), who provided a comprehensive mathematical framework for the problem based on the study of the bifurcations of the system. The main control parameter defining the stability properties is the solar irradiance S^*. Below the critical value $S_{W\to SB}$, only the snowball state is permitted, whereas above the critical value $S_{SB\to W}$, only the warm state is permitted. Such critical values, which determine the region of bistability, are defined by bifurcations that emerge when, roughly speaking, the strength of the positive, destabilising feedbacks becomes as strong as the negative, stabilizing feedbacks.

Only later these predictions were confirmed by actual data. Indeed, geological and paleomagnetic evidence suggests that during the Neoproterozoic era, between 630 and 715 million years ago, the Earth went at least twice into major long-lasting global glaciations that can be associated with the SB state; see Pierrehumbert et al. (2011) and Hoffman et al. (1998). Multicellular life emerged in our planet shortly after the final deglaciation from the last SB state (Gould, 1989). The robustness and importance of the competition between the Bolzmann feedback and the ice-albedo feedback in defining the global stability properties of the climate has been confirmed by investigations performed using higher complexity models (Lucarini et al., 2010; Pierrehumbert et al., 2011), including fully coupled climate models (Voigt and Marotzke, 2010). While the mechanisms described above are pretty robust, the concentration of greenhouse gases as well as the boundary conditions defined by the extent and position of the continents have an impact on the values of $S_{W\to SB}$ and $S_{SB\to W}$ as well as on the the properties of the competing states. The presence of multistability has a key importance in terms of determining habitability conditions for Earth-like exoplanets; see Lucarini et al. (2013) and Linsenmeier et al. (2015).

Additionally, several results indicate that the phase space of the climate system might well be more complex than the scenario of bistability described above. Various studies (Lewis et al., 2007; Abbot et al., 2011; Lucarini and Bódai, 2017; Margazoglou et al., 2021) performed with highly nontrivial climate models report the possible existence of additional competing states, up to a total of five (Brunetti et al., 2019; Ragon et al., 2021). In Margazoglou et al. (2021) it is argued that, in fact, one can see the climate as a multistable system where multistability is realised at different hierarchical levels. As an example, the tipping points (Lenton et al., 2008; Steffen et al., 2018) that characterise the current (W) climate state can be seen as a manifestation of a hierarchically lower multistability with respect to the one defining the dichotomy between the W and SB states.

https://doi.org/10.5194/npg-2021-34
Preprint. Discussion started: 5 November 2021


Nonlinear Processes in Geophysics
Discussions
Open Access
EGU

1.2 Transitions between Competing Metastable States: Gaussian vs Lévy Noise

Clearly, in the case of autonomous systems where the phase space is partitioned in more than one basin of attraction of the corresponding attractors and the basin boundaries, the asymptotic state of the system is determined by its initial conditions. Things change dramatically when one includes time-dependent forcing which allows for transitions between competing metastable states (Ashwin et al., 2012). In particular, following the viewpoint originally proposed by Hasselmann (1976), whereby the fast variables of the climate system act as stochastic forcings for the slow ones (Imkeller and von Storch, 2001), the relevance of studying noise-induced transitions between competing states has become apparent (Hänggi, 1986; Freidlin and Wentzell, 1984).

This viewpoint, where the noise is usually assumed to be Gaussian distributed, has provided very fruitful insight on the multiscale nature of climatic time series (Saltzman, 2001), and is related to the discovery of phenomena like stochastic resonance (Benzi et al., 1981; Nicolis, 1982). Metastability is ubiquitous in nature and advancing its understanding is a key challenge in complex system science at large(Feudel et al., 2018).

In general, the transitions between competing metastable states in stochastically perturbed multistable systems take place, in the weak noise limit, through special regions of the basin boundaries, named edge states. The edge states are saddles: trajectories initialised in the basin boundaries are attracted to them, but there is an extra direction of instability, so that a small perturbation sends an orbit towards one of the competing metastable states with probability one (Grebogi et al., 1983; Ott, 2002; Kraut and Feudel, 2002; Skufca et al., 2006; Vollmer et al., 2009). In previous papers, we have shown that it is possible to construct edge states in high-dimensional climate models Lucarini and Bódai (2017) and to prove that the population of each metastable state and the statistics of the noise-induced transitions can be understood (Lucarini and Bódai, 2019; Lucarini and Bódai, 2020; Margazoglou et al., 2021) by considering the nonequilibrium quasi-potential formalism introduced by Graham (1987) and Graham et al. (1991). In the case the edge state supports chaotic dynamics, we refer to it as Melancholia (M) state (Lucarini and Bódai, 2017). The local minima and the saddles of the quasi-potential Φ, which generalises the classical energy landscape for non-gradient systems, correspond to competing metastable states and to edge states, respectively. The system is forced by adding a random - Gaussian distributed - component to the solar irradiance, which impacts, in the form of multiplicative noise, only a small subset of the degrees of freedom of the system. We remark that such choice of the stochastic forcing does not fully reflect physical realism, as the variability of the solar irradiance has a more complex behaviour (Solanki et al., 2013). Instead, noise acts as a tool for exploring the global stability properties of the system, and injecting noise as fluctuation of the solar irradiance has the merit of impacting the Lorenz energy cycle, thus effecting all degrees of freedom of the system (Lucarini and Bódai, 2020).

A major limitation of this mathematical framework is the need to rigidly consider Gaussian noise laws, even if considerable freedom is left as to the choice of the spatial correlation properties of the noise. Following Ditlevsen (1999), it has become apparent that white noise is not the only meaningful option for trying to model noise-induced transitions in the climate system, while, instead, more general classes of α-stable Lévy noise laws might be useful for explaining the observed phenomena. Lévy processes (Applebaum, 2009; Duan, 2015), described in detail below in Appendix A, provide a powerful framework

https://doi.org/10.5194/npg-2021-34
Preprint. Discussion started: 5 November 2021


Nonlinear Processes in Geophysics Discussions

for understanding ultrarapid transitions. Note that the stability parameter $\alpha \in (0,2]$, where the $\alpha = 2$ case corresponds to the Gaussian case (which is, indeed, a special Lévy process). In what follows, when we discuss Lévy noise laws, we refer to $\alpha \in (0,2)$.

The proposal by Ditlevsen stimulated mathematical investigations into noise-induced escapes from attractors where as stochastic forcing one chooses a Lévy, rather than Gaussian, noise (Imkeller and Pavlyukevich, 2006a, b; Chechkin et al., 2007; Debussche et al., 2013). Such analyses have clarified that a fundamental dichotomy exists with the classical Freidlin and Wentzell scenario mentioned above, even if phenomena like stochastic resonance can be recovered also in this case (Dybiec and Gudowska-Nowak, 2009; Kuhwald and Pavlyukevich, 2016). Whereas in the Gaussian case transitions between competing attractors occur as a result of the very unlikely combination of many steps all going in the *right* direction, in the Lévy case, transitions result from individual, very large and very rare jumps. Recently, Duan and collaborators have made fundamental progresses in achieving a variational formulation of Lévy noise-perturbed dynamical systems (Hu and Duan, 2020) as well as in developing corresponding methods for data assimilation (Gao et al., 2016) and data analysis (Lu and Duan, 2020). In terms of applications, Lévy noise is becoming a more and more a popular concept and tool for studying and interpreting complex systems (Grigoriu and Samorodnitsky, 2003; Penland and Sardeshmukh, 2012; Zheng et al., 2016; Wu et al., 2017; Serdukova et al., 2017; Cai et al., 2017; Singla and Parthasarathy, 2020; Gottwald, 2021).

The contribution (Gottwald, 2021) is especially worth recapitulating because of its methodological clarity. There, the idea is, following Ditlevsen (1999), to provide a conceptual deterministic climate model able to generate a Lévy-noise-like signal to describe, at least qualitatively, abrupt climate changes similar to Dansgaard–Oeschger events, which are sequences of periods of abrupt warming followed by slower cooling that occurred during the last glacial period (Barker et al., 2011). A key building block is the idea proposed in Thompson et al. (2017) that a Lévy noise can be produced by integrating the so-called correlated additive and multiplicative (CAM) noise processes, which are defined starting from standard Gaussian processes. The other key ingredient is to consider the atmosphere as the fast component in the multiscale model and deduce, using homogeneization theory (Pavliotis and Stuart, 2008; Gottwald and Melbourne, 2013), that its influence on the slower climate components can be closely represented as a Gaussian forcing. Finally, the temperature signal is cast as the integral of a CAM process.

1.3 Outline of the Paper and Main Results

We consider here the Ghil-Sellers Earth's EBM (Budyko, 1969; Sellers, 1969; Ghil, 1976), a diffusive one-dimensional energy balance system, governed by a nonlinear reaction-diffusion parabolic partial differential equation. We stochastically perturb the system by adding random fluctuations to the solar irradiance, therefore the noise is introduced in multiplicative form. We study the transitions between the two competing metastable climate states and carry out a comparison of the effect of considering Lévy vs Gaussian noise laws of weak intensity ε.

The paleoclimatic records indicate that abrupt climate changes like Dansgaard–Oeschger events have a strong non-Gaussian heavy-tailed distribution and discontinuous càdlàg paths, thus motivating scientists to model noise-induced transitions in the climate system considering α-stable Lévy process as a source of the stochastic perturbation (Ditlevsen, 1999; Dakos et al., 2008; Corral and González, 2019).

https://doi.org/10.5194/npg-2021-34
Preprint. Discussion started: 5 November 2021


Nonlinear Processes in Geophysics
Discussions
Open Access
EGU

The main challenges of the problem are: a) the fact that we are considering dynamical processes occurring in infinite dimensions (Doering, 1987; Duan and Wang, 2014; Alharbi, 2021); and b) the consideration of multiplicative Lévy noise laws (Løkka et al., 2004; Peszat and Zabczyk, 2007; Debussche et al., 2013). We characterize noise-induced transitions between the competing climate basins and quantify the effect of noise parameters on them by estimating the statistics of escape times and empirically constructing mean transition pathways called instantons.

The results obtained confirm that, in the weak noise limit $\varepsilon \to 0$, the mean residence time in each metastable state driven by Gaussian vs. Lévy noise has a fundamentally different dependence on ε. Indeed, as expected, in the Gaussian case the residence time grows exponentially with ε^{-2}, thus in basic agreement with the well-known Kramers (1940) lsaw and the previous studies performed on climate models (Lucarini and Bódai, 2019; Lucarini and Bódai, 2020). Instead, in the case of α-stable noise laws, the residence time increases with $\varepsilon^{-\alpha}$. We perform simulations for $\alpha = \{0.5, 1.0, 1.5\}$. The obtained scaling is in agreement with what is found for low dimensional dynamics (Imkeller and Pavlyukevich, 2006a, b), as well as with the infinite dimensional stochastic Chafee-Infante reaction-diffusion equation (Debussche et al., 2013) in the case of additive noise. This might indicate that such scaling laws are more general than what typically considered.

Furthermore, we find clear confirmation that, in the case of Gaussian noise in the weak noise limit, the escape from either attractor's basin takes place through the edge state. Indeed, the most probable paths for both thawing and freezing processes meet at the edge state and have distinct instantonic and relaxation sections. In turn, for Lévy noise in the weak-noise limit, the escapes from a given basin of attraction occur through the boundary region closest to the outgoing attractor. Hence, the paths are very different from the Gaussian case (especially so for the freezing transition) and, somewhat surprisingly, are identical regardless the value of α considered.

The rest of the paper is organized as follows. In Section 2 we present the Ghil-Sellers EBM and summarize its most important dynamical aspects, as well as the steady-state solutions and their stability. The stochastic partial differential equation obtained by randomly perturbing the solar irradiance in the EBM is given in Subsection 3.1, where we also clarify the mathematical meaning of the solution of the stochastic partial differential equation. Subsection 3.2 introduces the mean residence time and most probable transition path between the competing climate states. The numerical methods are also briefly presented. In Section 4 we present and discuss our main results. The comparative analysis of the impact of stochastic forcing due to Gaussian vs Lévy noise is carried out in two directions: taking into account the mean residence time and the mean transition paths between the attractors. Finally, Appendix A presents a succinct description of α-stable Lévy processes, Appendix B sketches the derivation of the scaling laws for mean residence times presented in Debussche et al. (2013), and Appendix C presents a tabular summary of the statistics of the problem.

2 The Ghil-Sellers energy balance climate model

The Ghil-Sellers EBM is described by an one-dimensional nonlinear, parabolic, reaction-diffusion partial differential equation (PDE) (1) involving the surface temperature T field and the transformed space variable $x = 2\phi/\pi \in [-1, 1]$, where

https://doi.org/10.5194/npg-2021-34
Preprint. Discussion started: 5 November 2021


Nonlinear Processes in Geophysics
Discussions
Open Access
EGU

$\phi \in [-\pi/2, \pi/2]$ is the latitude

$$C(x)T_t = \frac{4}{\pi^2 \cos(\pi x/2)}[\cos(\pi x/2)K(x,T)T_x]_x + \mu Q(x)[1-\alpha_a(x,T)] - \sigma T^4[1-m\tanh(c_3 T^6)], \tag{1}$$

where C is the effective heat capacity, and $T = T(x,t)$ has boundary and initial conditions as follows

$$T_x(-1,t) = T_x(1,t) = 0, \qquad T(x,0) = T_0(x). \tag{2}$$

The equation does not depend explicitly on the time t. The subscripts $_t$ and $_x$ refer to partial differentiation. The first term - D_I - on the right hand side of (1) describes the meridional heat transport on the Earth's surface, where function $K(x,T)$ is a combined diffusion coefficient, given by

$$K(x,T) = k_1(x) + k_2(x)g(T), \text{ with} \tag{3}$$

$$g(T) = \frac{c_4}{T^2}\exp\left(-\frac{c_5}{T}\right). \tag{4}$$

The empirical functions $k_1(x)$ and $k_2(x)$ are eddy diffusivities for sensible and latent heat, respectively. The second term - D_{II} - of (1) describes the heat absorption controlled by the incoming solar radiation $Q(x)$ as modulated by the surface reflectivity (albedo) $\alpha_a(x,T)$, given by

$$\alpha_a(x,T) = \{b(x) - c_1(T_m + \min[T - c_2 z(x) - T_m,\ 0])\}_c, \tag{5}$$

where the subscript $\{\cdot\}_c$ denotes a cutoff for a generic quantity h defined as

$$h_c = \begin{cases} h_{min} & h \le h_{min}, \\ h & h_{min} < h < h_{max}, \\ h_{max} & h_{max} \le h. \end{cases} \tag{6}$$

The term $c_2 z(x)$ in (5) indicates the difference between the sea-level and surface-level temperatures, and $b(x)$ is a temperature independent empirical function of the albedo. The parametrization given in Eqs. (5)-(6) encodes the positive ice-albedo feedback. The relative intensity of the solar radiation in the model can be controlled by the parameter μ.

The last term - D_{III} - of (1) describes the energy loss to space by outgoing thermal planetary radiation and is responsible for the negative Boltzmann feedback. It is represented by the product of the Stefan-Boltzmann constant σ and of the emissivity coefficient $1 - m\tanh(c_3 T^6)$. Such term describes, in a simple yet effective way, the greenhouse effect by reducing infrared radiation losses. The values of the empirical functions $C(x), Q(x), b(x), z(x), k_1(x), k_2(x)$ at discrete latitudes and empirical constants $c_1, c_2, c_3, c_4, c_5, \sigma, m, T_m$ are taken from Ghil (1976), as modified in Bódai et al. (2015).

In this study, we consider $\mu = 1.05$. For this value of μ, two stable asymptotic states - the W and the SB states - co-exist, see Figure 1(b), reproduced from Bódai et al. (2015). Indeed, a codimension one manifold separates the basins of attraction of the W and SB states. We refer to D^W (D^{SB}) as the basin of attraction of the W (SB state). We refer to B as the basin boundary, which includes a single edge state M. Therefore, the system has three stationary solutions $T_W(x)$, $T_{SB}(x)$, and $T_M(x)$ for the W,

https://doi.org/10.5194/npg-2021-34
Preprint. Discussion started: 5 November 2021

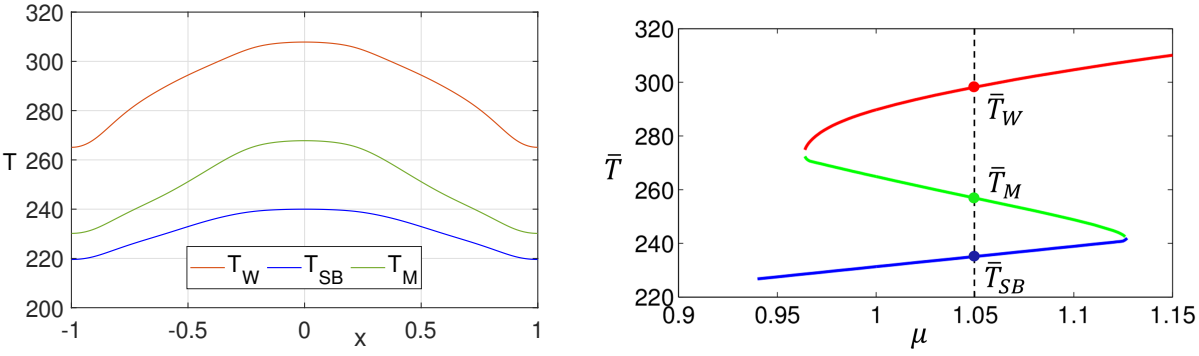

Figure 1. (a) Stationary solutions $T_W(x)$, $T_{SB}(x)$ and $T_M(x)$ in Kelvin (K) of zonally averaged energy-balance model (1). (b) Bifurcation diagram of the average temperature $\overline{T}$ as a function of control parameter μ, adapted from Bódai et al. (2015).

SB, and M state, respectively, shown in Figure 1(a). In Ghil (1976) the three stationary solutions were obtained by equating T_t to 0, and it was shown, through linear stability analysis, that the stationary solutions T_W and T_{SB} are stable, while T_M is unstable. In Bódai et al. (2015) the unstable solution T_M was constructed using a modified version of the edge tracking algorithm Skufca et al. (2006).

Following previous studies (Bódai et al., 2015; Lucarini and Bódai, 2019; Lucarini and Bódai, 2020; Margazoglou et al., 2021), when visualising our results, we apply a coarse-graining to the phase space of the model. In what follows, we perform a projection on the plane spanned by the spatially averaged temperature $\overline{T}$ and the averaged Equator minus Poles temperature difference ΔT, defined as

$$\overline{T} = [T(x,t)]_0^1, \tag{7}$$

$$\Delta T = [T(x,t)]_0^{1/3} - [T(x,t)]_{1/3}^1, \text{ where} \tag{8}$$

$$[T(x,t)]_{x_l}^{x_h} = \frac{\int_{x_l}^{x_h} \cos(\pi x/2) T(x,t) dx}{\int_{x_l}^{x_h} \cos(\pi x/2) dx}. \tag{9}$$

Such a representation allows for a minimal yet still physically relevant description of the system. Indeed, changes in the energy budget of the system (warming versus cooling) are, to a first approximation, related to variations in $\overline{T}$, while the large-scale energy transport performed by the geophysical fluids is controlled by ΔT. The boundary between high and low latitude in (8) is established at $x = \pm 1/3$, i.e. at $30°N/S$. Additionally, in some visualizations, we consider as a third coordinate the fraction of the surface with a below-freezing temperature (therefore we expect 1 for global glaciation and 0 for no ice). We refer to this variable as I, and it is an attempt to extract an observable that resembles the sea-ice percentage of the Earth's surface. Thus, the stationary solutions $T_W(x)$, $T_{SB}(x)$, and $T_M(x)$, in terms of ΔT and $\overline{T}$, correspond to $\Delta T_W = 16$ K, $\Delta T_{SB} = 8.3$ K, $\Delta T_M = 17.5$ K; $\overline{T}_W = 297.7$ K, $\overline{T}_{SB} = 235.1$ K, $\overline{T}_M = 258$ K; and $I_W = 0.2$, $I_{SB} = 1$, and $I_M = 1$.

https://doi.org/10.5194/npg-2021-34
Preprint. Discussion started: 5 November 2021

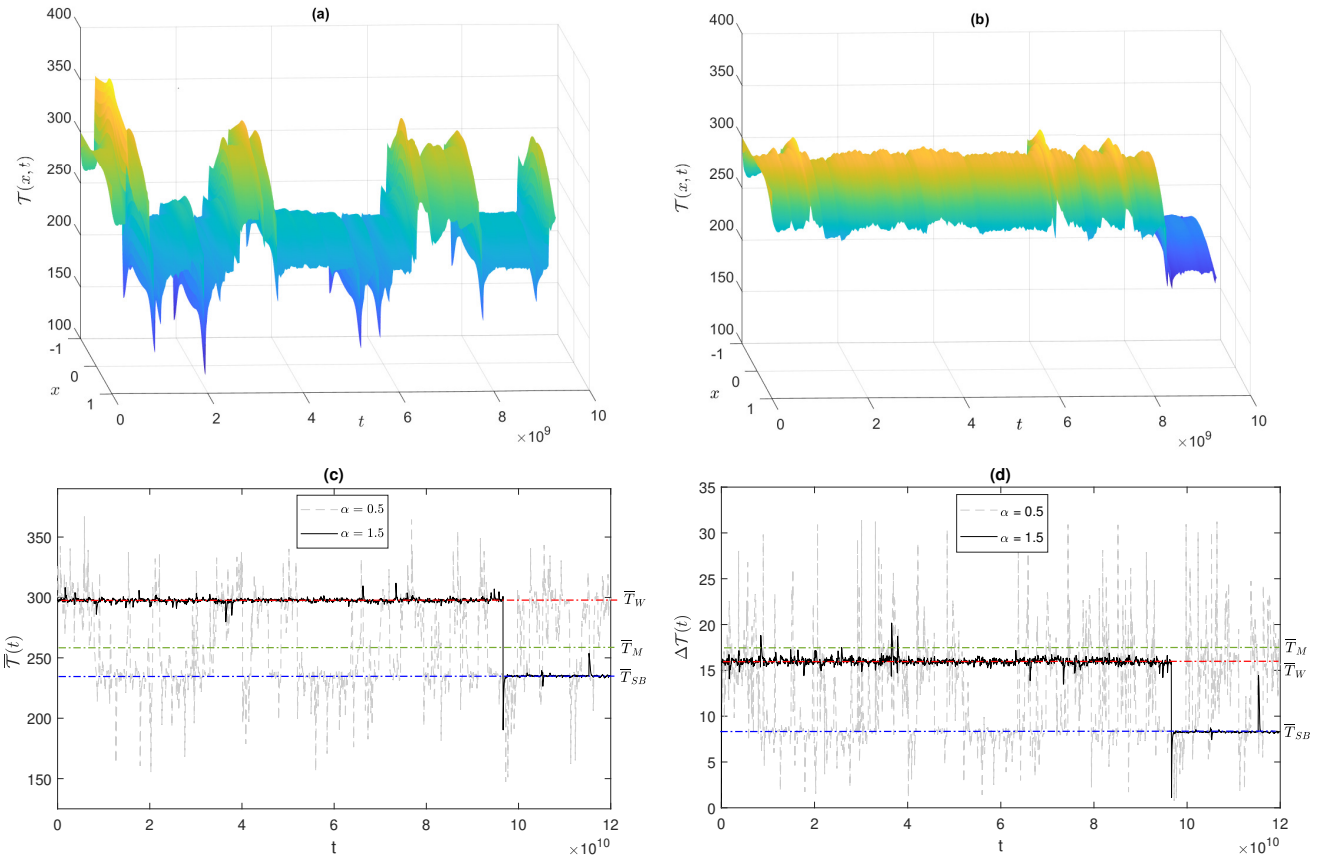

Figure 2. The metastable behavior of solution path of stochastic energy-balance model (10) for $\varepsilon = 0.04$, $T_0 = 300$ K, $t \in (0, 300)$ years (a) $\alpha = 0.5$, (b) $\alpha = 1.5$ and of (c) temperature average $\overline{\mathcal{T}}$ and (d) temperature contrast at low and high latitudes $\Delta\mathcal{T}$ for $\varepsilon = 0.01$, $\alpha = 0.5, \alpha = 1.5$. Red/green/blue dashed-dotted lines portray stationary climate states $\overline{T}_W/\overline{T}_M/\overline{T}_{SB}$, respectively.

3 Background and Methodology

3.1 Stochastic Energy Balance Model.

In order to analyze the influence of random perturbations on the deterministic dynamics of the climate model described in Section 2, we perturb the relative intensity μ of solar radiation by a symmetric α-stable Lévy process and rewrite Eq. (1) in the form of the following stochastic partial differential equation (SPDE)

$$C(x)\mathcal{T}_t = D_I(x,\mathcal{T},\mathcal{T}_x,\mathcal{T}_{xx}) - D_{III}(\mathcal{T}) + \mathcal{Q}(x)[1-\alpha_a(x,\mathcal{T})][\mu + \varepsilon \dot{L}^{\alpha}(t)], \tag{10}$$

with boundary and initial conditions defined by Eq. (2) where $\mathcal{T}$ is the evolving stochastic temperature field.

https://doi.org/10.5194/npg-2021-34
Preprint. Discussion started: 5 November 2021

Nonlinear Processes in Geophysics
Discussions
Open Access
EGU

Here the parameter $\varepsilon > 0$ controls the noise intensity and $(L^{\alpha}(t)_{t\geq 0})$ is a symmetric α-stable process defined in Appendix A. As mentioned before, we refer to the Lévy case if the stability parameter $\alpha \in (0,2)$, so that we consider a jump process. We recall that the jumps become more frequent and less intense as α increases.

We define $\dot{\mathcal{L}}(t) = \mathcal{Q}(x)[1-\alpha_a(x,\mathcal{T})]\dot{L}^{\alpha}(t)$, as the generalised derivative of a stochastic process in a suitably defined functional space. Equation (10) features multiplicative noise. The research interest on this type of SPDEs (Løkka et al., 2004; Doering, 1987; Peszat and Zabczyk, 2007; Duan and Wang, 2014; Alharbi, 2021) is mainly focused on defining weak, strong, mild, and martingale solutions, and in specifying under which conditions these solutions exist and are unique, and in constructing numerical approximation schemes for the solutions (Davie and Gaines, 2000; Cialenco et al., 2012; Burrage and Lythe, 2014; Jentzen and Kloeden, 2009; Kloeden and Shott, 2001), among other aspects.

First let us define the concept of mild solution in this context. Let $(\Omega, \mathcal{F}, \mathbb{P})$ be a given complete probability space and $H(\|\cdot\|, \langle\cdot,\cdot\rangle)$ a separable Hilbert space with norm $\|\cdot\|$ and inner product $\langle\cdot,\cdot\rangle$. Equation (10) can be rewritten in the more general form as follows

$$\begin{aligned} &\mathcal{T}_t = A(x)\,[E(x,\mathcal{T})\,\mathcal{T}_x]_x + F(x,\mathcal{T}) + \varepsilon G(x,\mathcal{T})\dot{L}^{\alpha}(t), \\ &\mathcal{T}_x(-1,t) = \mathcal{T}_x(1,t) = 0, \\ &\mathcal{T}(x,0) = T_0(x), \end{aligned} \tag{11}$$

where A, E, F, G are Lipschitz functions defined on $[-1,1]\times H$ and $G(x,\mathcal{T})\dot{L}^{\alpha}(t) = \dot{\mathcal{L}}(t)$. Under certain assumptions (Yagi, 2009), the problem (11) is formulated as a Cauchy problem whose local mild solution, a progressively measurable process $\mathcal{T}(t)$, for all $t \in [0, t_F]$ and $T_0 \in H$ has the following integral representation

$$\mathcal{T}(t) = \Psi(t)T_0 + \int_0^t \Psi(t-s)\Upsilon(\mathcal{T}(s))ds + \varepsilon\int_0^t \Psi(t-s)G(\mathcal{T}(s))d\beta + \varepsilon\int_0^t \Psi(t-s)G(\mathcal{T}(s))d\gamma, \tag{12}$$

where the dependence on x is kept implicit and β (γ) is the Poisson random measure (compensated Poisson random measure) defined through Lévy-Itô decomposition. $\Psi(t)$, $t \geqslant 0$ is the evolution operator with the generalized semigroup property for the family of sector operators with the bounded inverses, and $\Upsilon(\mathcal{T}) = \mathcal{T} + F(x,\mathcal{T})$, $\mathcal{T} \in H$ is a nonlinear operator, which we assume Lipschitz to be continuous. Following the abstract theory presented in Yagi (2009), under certain structural assumptions for the operators Ψ and Υ and for the functional space, one can prove that the solution (12) is the unique local mild solution of Eq. (11). For illustrative reasons, some sample solutions for different values of α, simulated by the spatial discretization method (Skeel and Berzins, 1990) adapted to SPDEs, are shown in Figure 2 (a)-(b).

3.2 Noise-induced Transitions: Mean residence Times

By incorporating stochastic forcing into the system, its long-time dynamics change significantly, allowing transitions between the competing basins. This dynamical behaviour is called metastability, and is graphically captured by Figure 2, where in plots (a-b) a typical spatio-temporal evolution of the temperature field is shown, for stability parameters $\alpha = 0.5$ and $\alpha = 1.5$, respectively. Instead, in plots (c-d) the temporal noise-induced evolution of global temperature $\overline{\mathcal{T}}$ and the averaged Equator

https://doi.org/10.5194/npg-2021-34
Preprint. Discussion started: 5 November 2021


Nonlinear Processes in Geophysics
Discussions
Open Access
EGU

and Poles temperature difference $\Delta\mathcal{T}$ (as defined in Eqs. (7)-(8)) is shown for the same α. In what follows, we investigate the time statistics and the paths of the transitions between such basins.

In a complete probability space $(\Omega,\mathcal{F},\mathbb{P})$ we define the first exit time τ_x of a cádlág mild solution $\mathcal{T}(\cdot;x)$ of (10) starting at $x \in D^{W/SB}$ domain of warm/snowball climate stable state as

$$\tau_x(\omega) = \inf\{t > 0 | \mathcal{T}_t(\omega,x) \notin D^{W/SB}\}, \quad \omega \in \Omega,\ x \in H. \tag{13}$$

The mean residence time is then expressed by $\mathbb{E}[\tau_x(\omega)]$. In the case of the infinite dimensional multistable reaction-diffusion system described by Chafee-Infante equation under the influence of additive infinite-dimensional α-stable Lévy noise - $\alpha \in (0,2)$ - it was shown (Debussche et al., 2013) that in the weak-noise limit $\varepsilon \to 0$ the mean residence time in one of the competing basins of attraction increases as $\varepsilon^{-\alpha}$. For this time scale of ε the jump diffusion system reduces to a finite state Markov chain with values in the set of stable states. Details of this method are given in Appendix B. Similar results have been obtained for bistable one-dimensional SDEs (Imkeller and Pavlyukevich, 2006a, b).

As mentioned above, things are radically different for the special case $\alpha = 2$, which corresponds to Gaussian noise. In this case, we revisit Eq. (11) and we define $\dot{L}^{\alpha=2}(t) = \dot{W}(t)$, where $(W(t)_{t\geq 0})$ is a Wiener process. We then define $\dot{\mathcal{W}}(t) = G(x,\mathcal{T})\dot{W}(t)$ as the generalised derivative of a Wiener process in a suitably defined functional space. In the weak noise limit, one can express the statistics of transition times using large deviation laws (Varadhan et al., 1985). While the corresponding finite dimensional problem is thoroughly documented in the literature (Freidlin and Wentzell, 1984), and has been applied in a similar context by some of the authors (Lucarini and Bódai, 2019; Lucarini and Bódai, 2020; Ghil and Lucarini, 2020; Margazoglou et al., 2021), the treatment of infinite dimensional SDEs driven by an infinite dimensional Wiener process via the Freidlin-Wentzell theory requires further extension. In the present context, we refer to Budhiraja and Dupuis (2000) and Budhiraja et al. (2008) and references therein where the problem of an infinite dimensional reaction-diffusion equation driven by an infinite dimensional Wiener process has been addressed.

We assume that steady state conditions and ergodicity are met, and we also assume that the analysing system is bistable and a unique edge state is present at the basin boundary, as in the case studied here. One has that the mean residence time in either basin of attraction decreases exponentially with increasing noise intensity ε and is given by a generalized Kramers' law

$$\mathbb{E}[\tau_{W/SB}(\varepsilon)] \approx \exp\left(\frac{2\Delta\Phi_{W\to M/SB\to M}(\mathcal{T})}{\varepsilon^2}\right), \tag{14}$$

where $\Delta\Phi_{W\to M} = \Phi_M(\mathcal{T}) - \Phi_W(\mathcal{T})$ is the height of the quasi-potential barrier in the W attractor, and, correspondingly $\Delta\Phi_{SB\to M}(\mathcal{T}) = \Phi_M(\mathcal{T}) - \Phi_{SB}(\mathcal{T})$ is the height of the quasi-potential barrier in the SB attractor, and Φ is the Graham's quasi-potential mentioned above (Graham, 1987; Graham et al., 1991).

3.3 Noise-induced Transitions: Most Probable Transition Paths

In the weak noise limit, the most probable path to escape an attractor is defined by a class of trajectories named "instantons" (Grafke et al., 2015; Bouchet et al., 2016; Grafke et al., 2017; Grafke and Vanden-Eijnden, 2019) or maximum likelihood

https://doi.org/10.5194/npg-2021-34
Preprint. Discussion started: 5 November 2021


Nonlinear Processes in Geophysics
Discussions
Open Access
EGU

escape paths (Lu and Duan, 2020; Dai et al., 2020; Hu and Duan, 2020; Zheng et al., 2020).. However, considering different noise laws result into possibly radically different instantonic trajectories Dai et al. (2020); Zheng et al. (2020).

In our case, the theory indicates that if the stochastic forcing is Gaussian, under rather general hypothesis, the instanton will connect the attractor W/SB with the edge state M. Hence, M acts as gateway for noise induced transitions *if the noise is Gaussian*. Once the quasi-potential barrier is overcome, a free fall "relaxation" trajectory links M with the competing attractor SB/W. For equilibrium systems, (e.g. for gradient flows) where detailed balance is achieved, the relaxation and instantonic trajectories within the same basin of attraction are identical. On the contrary, for non-equilibrium systems, the relaxation and instantonic trajectories will differ, and will only meet at the attractor. See a detailed discussion of this aspect and of the dynamical interpretation of the quasi-potential Φ in Lucarini and Bódai (2020) and Margazoglou et al. (2021). Instead, if the noise is of Lévy type, the theory formulated for simpler equations suggests that the instanton will connect the attractor with a region on the basin boundary that is the nearest, in the phase space, to the attractor, as the concept of quasi-potential is immaterial (Imkeller and Pavlyukevich, 2006a, b; Imkeller and von Storch, 2001).

In general, the maximum likelihood transition trajectory $x_M(t)$ can be defined (Zheng et al., 2020; Lu and Duan, 2020) as a set of system states at each time moment $t \in [0, t_f]$ that maximizes the conditional probability density function $p(\,.\,|\,.\,;\,.\,)$ of passage from the origin stable state $\phi^{W/SB}$ to the destination stable state $\phi^{SB/W}$ and is expressed as

$$x_M(t) = \arg\max_x \left[p\left(\mathcal{T}(t) = x \,|\, \mathcal{T}(0) = x_0; \mathcal{T}(t_f) = x_f\right)\right] = \frac{p\left(\mathcal{T}(t_f) = x_f \,|\, \mathcal{T}(t) = x\right) \cdot p\left(\mathcal{T}(t) = x \,|\, \mathcal{T}(0) = x_0\right)}{p\left(\mathcal{T}(t_f) = x_f \,|\, \mathcal{T}(0) = x_0\right)}, \tag{15}$$

where x_0 (x_f) belongs to the basin of attraction $D^{W/SB}$ ($D^{SB/W}$) and $p\,(\,.\,|\,.\,)$ is the probability density function evolving according to the Fokker-Planck equation (Risken, 1996). This method is applicable either if efficient numerical algorithms are available to solve the Fokker-Planck equation associated to the studied stochastically driven system, or, empirically, when considering a large ensemble of simulations. Note that this is not an asymptotic approach, i.e. it does not require a weak noise limit $\varepsilon \to 0$ for its application and is applicable for systems with either Gaussian or non-Gaussian noise. Yet, in the weak-noise limit, the definition (15) leads to constructing the optimal transition paths described above.

In the following section, for practical purposes, we construct such optimal transition path in the coarse grained 2D phase space $(\overline{\mathcal{T}}, \Delta\mathcal{T})$ and 3D phase space $(\overline{\mathcal{T}}, \Delta\mathcal{T}, \mathcal{I})$ of the variables defined in Sect. 2 by averaging the ensemble of transitions connecting the two competing states in the weak noise limit.

3.4 Numerical Methods

We solve Eq. (10) through the Matlab *pdepe* function, which is well suited for solving 1D parabolic and elliptic PDEs. We discretize the 1D space with a regular grid of 201 gridpoints, following Bódai et al. (2015).

The time span of integration $t \in [0, T_f]$, varies for different cases, with $T_f \in (10^5, 15 \cdot 10^5)$ years, with time stepping of one year. Each year, we consider a different value for the relative solar irradiance by extracting a random number Z_j, see Eq. (16). To simulate the stochastic noise term $\varepsilon L^\alpha(t)$, which is added in the parameter μ in Eq. (10), we use the recursive algorithm

https://doi.org/10.5194/npg-2021-34
Preprint. Discussion started: 5 November 2021


Nonlinear Processes in Geophysics
Discussions
Open Access
EGU

from Duan (2015). The process values $L^\alpha(t_1),...,L^\alpha(t_N)$ at each moment t_j, $j \in \mathbb{N}$, are obtained via

$$L^\alpha(t_j) = L^\alpha(t_{j-1}) + (t_j - t_{j-1})^{\frac{1}{\alpha}} Z_j, \qquad j = 1,...,N, \tag{16}$$

where the second term is an independent increment and Z_j are the independent standard symmetric α-stable random numbers generated by an algorithm in Weron and Weron (1995). See also Grafke et al. (2015) for a detailed explanation of the steps above. For the numerical simulations discussed below, we consider $\alpha = (0.5, 1.0, 1.5, 2)$ and $\varepsilon \in (0.0001, 0.3)$. We select ε in such a way that the noise intensity is strong enough to induce at least order of 10 transition, given our constraints in the time length of the simulations, and weak enough that we are not far from the weak-noise limit, where the scaling laws discussed above apply and transitions paths are well-organized. Our simulations are performed taking the Itô interpretation for the stochastic equations.

We remark that when we consider Lévy noise, it does happen that for some years the solar irradiance has negative values. Of course these conditions bear no physical relevance. Nonetheless, we have allowed for this to occur in our simulations in order to be able to stick to the desired mathematical framework. We remind that this study does not aim at capturing with any high degree of realism the description of the actual evolution of climate.

4 Results and Discussion

In what follows we aim at addressing three main questions: 1. What is the temporal statistics of the $SB \to W$ and $W \to SB$ transitions? 2. What are the typical transition pathways? 3. What are the fundamental differences between transitions caused by Gaussian vs. Lévy noise? A summary of the results of the numerical simulations is given in Table A1 in Appendix C, including sample size, i.e. number of transitions, point estimates for mean escape time and its 0.95-confidence intervals for exits from both W/SB stable basins. See the Data Availability section for information on how to access the supplementary material (Lucarini et al., 2021) containing the raw data produced in this study as well as some illustrative animations portraying noise-induced transitions between the two competing metastable states.

4.1 Mean Residence Time

Our analysis confirms that there is fundamental dichotomy in the statistics of mean residence times between Lévy noise and Gaussian noise-induced transitions.

Fig. 3(a) shows the dependence of the mean residence time in either attractor on ε and α for the Lévy case. The red circles correspond to permanence in the W basin, while the blue squares in the SB basin; see Lucarini et al. (2021) for additional details on the practical steps. The predicted scaling Eq. (B6) is shown by the dotted black line for each α. We also portray the best power law fit of the mean residence time with respect to ε for each value of α; the confidence intervals of the exponent is shown in Table 1. Our empirical results seem to indicate, at least in this case, an agreement with the $\varepsilon^{-\alpha}$ scaling presented in Eq. (B6) and discussed earlier in the paper. This points at the possibility that the $\varepsilon^{-\alpha}$ scaling might apply in more general conditions than what has been as of yet rigorously proven, and specifically when multiplicative Lévy noise is considered. The

https://doi.org/10.5194/npg-2021-34
Preprint. Discussion started: 5 November 2021

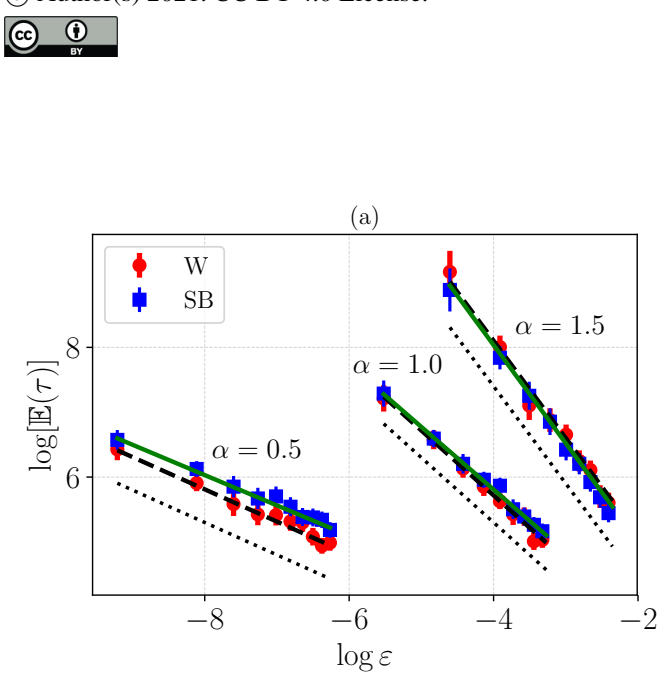

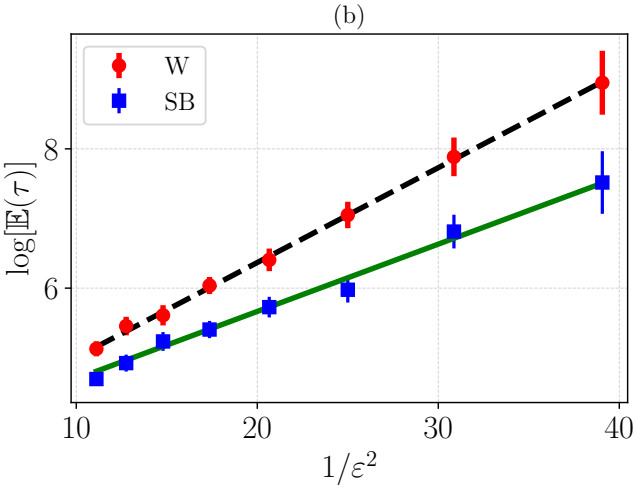

Figure 3. Estimates of the mean residence time $\mathbb{E}(\tau)$ in years inside the W (blue circles) and SB (red squares) states as a function of the noise intensity ε. (a) Lévy noise for $\alpha = 0.5$, 1.0, 1.5, with the dotted line being the corresponding prediction from Eq. (B6), while the straight green (SB) and dashed black (W) are the fittings of Eq. (B6) of the relevant dataset. (b) Gaussian noise, with straight green (SB) and dashed black (W) being the fit of Eq. (14).

Table 1. Estimates of exponent α via fitting of Eq. (B6) for the Lévy case (three first columns) and of energy barrier $\Delta\Phi_{\mathrm{W/SB}\to\mathrm{M}}$ via fitting of Eq. (14) for the Gaussian case (last column). In parenthesis is the estimated error of the last digit.

	Lévy			Gaussian
α	0.5	1.0	1.5	2
W	0.50(2)	1.00(2)	1.50(1)	$\Delta\Phi_{\mathrm{W}\to\mathrm{M}} = 0.068(1)$
SB	0.47(2)	0.97(2)	1.52(4)	$\Delta\Phi_{\mathrm{SB}\to\mathrm{M}} = 0.048(3)$

stochastically perturbed trajectories forced by Lévy noise consist of jumps, and the probability of occurrence of a high jump, which can trigger the escape from the reference basin of attraction, is polynomially small in noise intensity ε.

The Gaussian case - where no jumps are present - is portrayed in Fig. 3(b). We show in semi-logarithmic scale the mean residence time versus $1/\varepsilon^2$. We perform a successful linear fit of the logarithm of the mean residence time in either attractor versus $1/\varepsilon^2$, and using Eq. (14), we obtain an estimate of the local quasi-potential barrier $\Delta\Phi_{\mathrm{W/SB}\to\mathrm{M}}$, which is half of the slope of the corresponding straight lines of the linear fit; see the last column of Table 1. We conclude that for $\mu = 1.05$ the W basin of attraction has a deeper minimum of Φ than the SB one.

https://doi.org/10.5194/npg-2021-34
Preprint. Discussion started: 5 November 2021

Nonlinear Processes in Geophysics
Discussions
Open Access
EGU

4.2 Escape Paths for the Noise-Induced Transitions

We now explore the geometry of the transition paths associated with the metastable behaviour of the system. We first discuss the case of Gaussian noise because it is indeed more familiar and more extensively studied.

4.2.1 Gaussian noise

We estimate the transition paths by averaging among the escape plus relaxation trajectories using the run performed with the weakest noise, see Table A1. We first perform our analysis in the 2D-projected state space defined by $(\overline{\mathcal{T}}, \Delta\mathcal{T})$. We prescribe two small circular-shaped regions enclosing the two deterministic attractors and search the timeseries of the portions of the whole trajectory that leave one of such regions and reach the other one. This creates two subsets of our full dataset, from which we build a 2D histogram for each of the SB→W and W→SB transitions in the projected space. We then estimate the most probable transition paths by finding for each bin value of $\overline{\mathcal{T}}$ the peak of histogram in the $\Delta\mathcal{T}$ direction. The distributions are very peaked, and almost the same result is obtained by computing the average of $\Delta\mathcal{T}$ according to the 2D histogram conditional on the value of $\overline{\mathcal{T}}$.

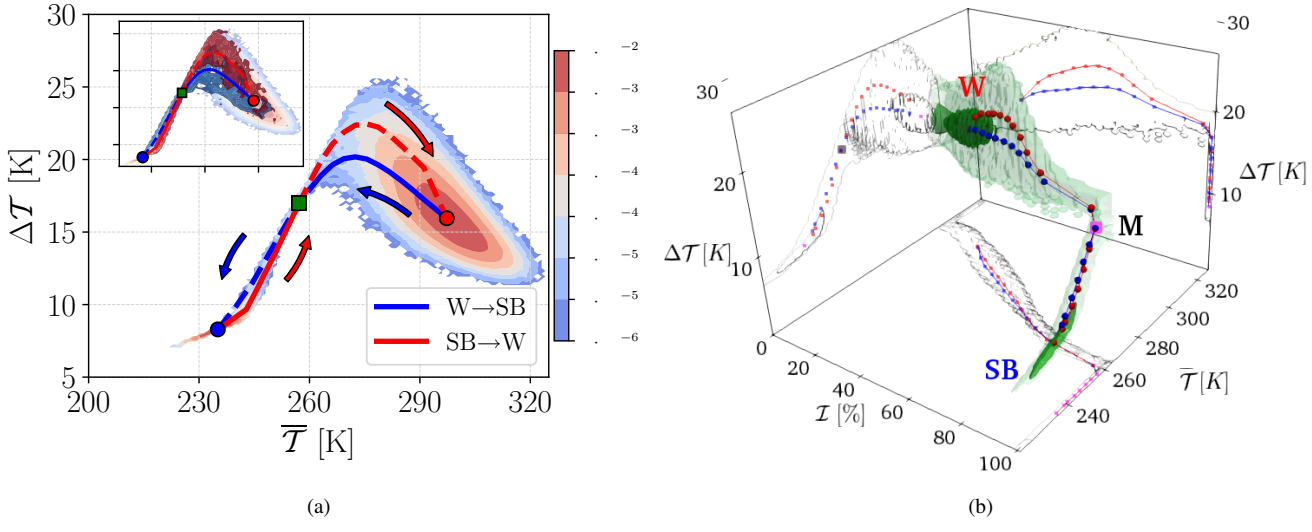

(a) (b)

Figure 4. (a) Invariant measure in the 2D-projected state space defined by $(\overline{\mathcal{T}}, \Delta\mathcal{T})$. The colored points indicate the deterministic attractors of the SB(blue) M(green) and W(red) states and the blue (red) line is the stochastically averaged transition paths for the $W \to SB$ ($SB \to W$) transitions. Dashed (solid) lines are the relaxation (instantonic) trajectories. The arrows show the direction of transitions. Top left inset: The dark blue (red) contours portray the ensembles of the transition paths between $W \to SB$ ($SB \to W$). Here the system is driven by Gaussian noise with $\varepsilon = 0.14$. (b) Invariant measure and most probable transition paths ($W \to SB$ in blue and $SB \to W$ in red) in the 3D-projected state space defined by $(\overline{\mathcal{T}}, \Delta\mathcal{T}, \mathcal{I})$. The darker green shading indicates higher probability density for the corresponding isosurface. A 2D projection in each plane is shown. The location of the M state is given by a pink square. Here the system is driven by Gaussian noise with $\varepsilon = 0.16$.

https://doi.org/10.5194/npg-2021-34
Preprint. Discussion started: 5 November 2021


Nonlinear Processes in Geophysics Discussions
Open Access
EGU

In the background of Fig. 4 (a) we show the empirical estimate of the invariant measure in the 2D-projected state space defined by $(\overline{\mathcal{T}}, \Delta\mathcal{T})$. Additionally, we indicate the position of the deterministic attractors, (SB-blue and W-red circles) and of the M state (green rectangle). In the inset of Fig. 4 (a) we present the ensemble of W→SB (SB→W) transitions as deep blue (red) contours. The most probable transition paths are shown in blue for the W→SB and in red for the SB→W. The instantonic portion of the blue (red) line is the one connecting the W (SB) attractor to the M state and is portrayed as a solid line, while the relaxation portion, connecting the M state with the SB (W) attractor, is portrayed as a dashed line. Within each basin of attraction, the instantonic and relaxation trajectories do not coincide, and, instead, only meet at the corresponding attractor and at the M state. This is particularly clear for the W state. The presence of such a loop is a signature of non-equilibrium dynamics, which was also observed in Margazoglou et al. (2021) and has, instead, gone undetected in Lucarini and Bódai (2019); Lucarini and Bódai (2020). See the supplementary material for some illustrative simulations of the transitions.

Let's provide some physical interpretation of how the transitions occur. Looking at the $SB \rightarrow W$ most probable path, the escape includes a simultaneous increase in ($\overline{\mathcal{T}}$ and $\Delta\mathcal{T}$). In practice, a $SB \rightarrow W$ transition takes place when, starting at the SB state, one has a (rare) sequence of positive anomalies in the fluctuating solar irradiance $\widetilde{\mu}$, i.e. $\widetilde{\mu} > \mu$. While the planet is warming globally, the Equator is warming faster than the Poles, resulting in a positive rate $\Delta\dot{\mathcal{T}} > 0$, because it receives, in relative and absolute terms, more incoming solar radiation. Hence, and considering that the Equator also in the SB state is warmer than the Poles, the melting of the ice occurs first at the Equator, with a subsequent decrease of the albedo in this latitude. Once the system crosses the M state, and supposing that persistent $\widetilde{\mu} < \mu$ do not appear at this stage, the system will relax towards the W state. The relaxation includes a consistent global warming of the planet, but with a change of sign in the rate of $\Delta\dot{\mathcal{T}}$, and a subsequent decrease of $\Delta\mathcal{T}$ implying that as soon as the temperature at the Equator has risen enough, the Poles will then warm at a faster pace, because the ice-albedo effect kicks in. The global freezing of the planet associated with the $W \rightarrow SB$ transition is qualitatively similar but not identical to the reverse $SB \rightarrow W$ process. Notice a considerable overlap of the transition paths ensembles in both basins of attraction, shown as red and blue contours in the inset of Fig. 4 (a). This implies a weakly non-equilibrium system, contrary to Margazoglou et al. (2021), where the $W \rightarrow SB$ and $SB \rightarrow W$ transitions occurred through fundamentally different paths; see discussion therein.

Figure 4 (b) presents the optimal transition paths $W \rightarrow SB$ and $SB \rightarrow W$ in a three dimensional projection where we add as third coordinate the variable $\mathcal{I}$, which indicates the fraction of the surface that has subfreezing temperatures ($\mathcal{T} < 273.15$ K). One of the 2D projections included in Fig. 4 (b) corresponds to the projection portrayed in Fig. 4 (a). Here, darker green shadings indicate higher density of points and the red and blue dots sample the highest probability for the $SB \rightarrow W$ and $W \rightarrow SB$ transitions paths, respectively. One could argue that the presence of an intersection between the $SB \rightarrow W$ and $W \rightarrow SB$ highest probability transition paths in Fig. 4 (a) could have been a simple effect of 2D projection. Instead, we see here that the $SB \rightarrow W$ and $W \rightarrow SB$ most probable transition paths also cross in the 3D projection in a well-defined region, which indeed corresponds to the M state (pink square).

https://doi.org/10.5194/npg-2021-34
Preprint. Discussion started: 5 November 2021

Nonlinear Processes in Geophysics
Discussions
Open Access
EGU

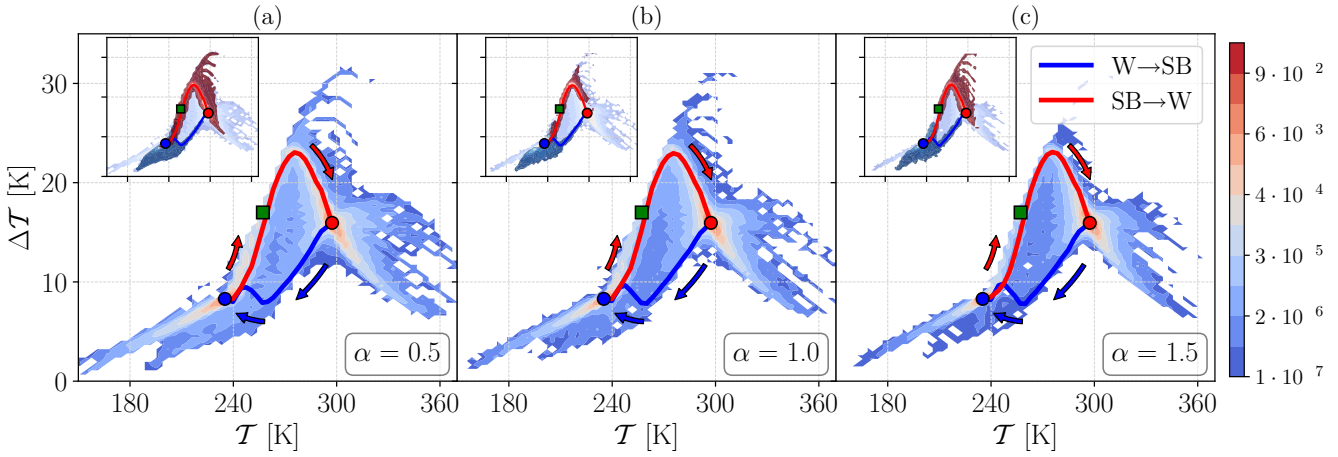

Figure 5. Two-dimensional projection of the invariant measure on $(\overline{\mathcal{T}}, \Delta\mathcal{T})$ for different choices of α for Lévy noise; (a) $\alpha = 0.5$ and $\varepsilon = 0.0001$, (b) $\alpha = 1$ and $\varepsilon = 0.004$, (c) $\alpha = 1.5$ and $\varepsilon = 0.01$. The blue (red) line corresponds to the W→SB (SB→W) most probable transition path, and the arrows show the direction of transitions. The colored points indicate the deterministic attractors of the SB(blue) M(green) and W(red) states. In the inset left top corner plot of (a-c) the dark blue (red) contours are the ensembles of the transition paths between $W \to SB$ ($SB \to W$).

4.2.2 Lévy noise

There is scarcity of rigorous mathematical results regarding the weak-noise limit of the transition paths between competing states in metastable stochastic systems forced by multiplicative Lévy noise. Indeed, the derivation of analytical results for this type of systems largely remains an open problem. Recently, for stochastic partial differential equations with additive Lévy and Gaussian noise, the Onsager-Machlup action functional has been derived in Hu and Duan (2020), leading to a precise formulation of the most probable transition paths. Hence, we do not have solid mathematical results to interpret what we describe below, where, instead, we need to use heuristic arguments. As far as we know, this is the first attempt to estimate the most probable transition pathway between the metastable states in infinite stochastic systems with multiplicative pure Lévy process.

A striking feature in Figure 5 is that the invariant measure and the structure of the most probable transition paths (SB→W and W→SB), in the weak-noise limit, are fundamentally different between the Lévy case and the Gaussian one. The invariant measure is highly peaked (dark red in the color scheme) in a small region around the deterministic attractors, as most typically the Lévy noise fluctuations of $\widetilde{\mu}$ are very small. Additionally, the most probable transition paths depend very weakly on the chosen value for the stability parameter α. This suggests that the geometry of most probable path of transitions does not depend on the frequency and height of the Lévy diffusion jumps, but rather on the qualitative fact that we are considering a discontinuous jump process. Note that each panel of Fig. 5 is computed using data coming from the weakest noise considered for the corresponding value of α.

https://doi.org/10.5194/npg-2021-34
Preprint. Discussion started: 5 November 2021

Nonlinear Processes in Geophysics
Discussions
Open Access
EGU

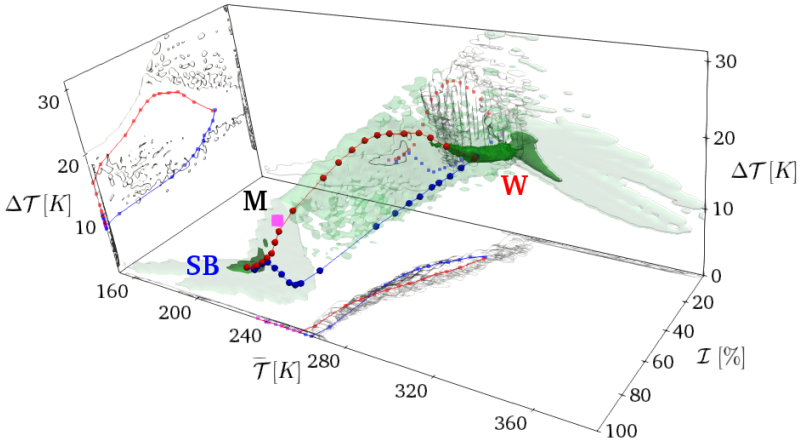

Figure 6. Same as Fig. 4 (b), but considering a stochastic forcing driven by a Lévy noise with $\alpha = 1.0$ and $\varepsilon = 0.004$.

The $W \rightarrow SB$ most probable transition path is characterized by the simultaneous decrease of both $\overline{\mathcal{T}}$ and $\Delta\mathcal{T}$. This implies that the jump process, causing the transition, leads to a rapid and direct freezing of the whole planet. The path crosses the basin boundary very far from the M state. Based on what is discussed in Sec. 3.2, we expect that the transition occurs through the nearest region to the outgoing attractor in the basin boundary.

The most probable $SB \rightarrow W$ transition follows, instead, a path that is somewhat similar to the one found for the Gaussian case. We then argue that the closest region in the basin boundary to SB attractor is in the vicinity of the M state. Note, that, nonetheless, the similarity between the Gaussian and Lévy case is less prominent when we look at 3D paths; compare Figs. 4(b) and 6. Indeed, in the Lévy case the $SB \rightarrow W$ path misses the M state. Further visual confirmation of the difference between the Gaussian and Lévy case can be found by looking at the animations included in the supplementary material.

5 Conclusions

It is a well-known that, as a result of the competition between the Boltzmann stabilizing feedback and the ice-albedo destabilizing feedback, under current astronomical and astrophysical conditions the climate system is multistable, as at least two competing and distinct climates are present, the W and the SB. More recent investigations indicate that the partition of the phase space of the climate system might be more complex, as more than two asymptotic states might be present, some of them, possibly, associated with small basins of attraction.

For deterministic multistable systems the asymptotic state of an orbit depends uniquely on the initial condition, and, specifically, on which basin of attraction it belongs to. The presence of stochastic forcing allows for transitions to occur between competing basins, thus giving rise to the phenomenon of metastability. Gaussian noise as a source of stochastic perturbations has been widely studied by the scientific community in recent years and provided very fruitful insight of the multiscale nature of the climatic time series. However it has become apparent that more general classes of α-stable Lévy noise laws might also

https://doi.org/10.5194/npg-2021-34
Preprint. Discussion started: 5 November 2021


Nonlinear Processes in Geophysics Discussions
Open Access
EGU

be suitable for modeling the observed climatic phenomena. In this regard, it is important to achieve a deeper understanding of the possible noise induced transitions between competing stable climate states under α-stable Lévy perturbations and compare them with the Gaussian case.

As a starting point in this direction, we have studied the influence of different noise laws on the metastability properties of the randomly forced Ghil-Sellers EBM, which is governed by a nonlinear, parabolic, reaction-diffusion PDE. In the deterministic version of the model, we have three steady-state solutions: two stable, attractive climate states and one unstable saddle, corresponding to the edge state. The stable states corresponds to the well-known W and SB climates. There is a fundamental dichotomy in the properties of the noise-induced transitions determined by whether we consider a stochastic forcing of intensity ε with a Gaussian versus an α-stable Lévy noise law. Note that, instead, the spatial structure of the noise is unchanged. This indicates that the phenomenology associated with the metastable behaviour depends critically on the choice of the noise law. Not many studies have investigated, numerically or through mathematical theory, the properties of transitions in metastable systems driven by multiplicative Lévy noise, as done here.

First, in the weak noise limit $\varepsilon \to 0$, the mean residence times inside either competing basin of attraction for diffusions driven by Gaussian vs. Lévy noise have a fundamentally different dependence on ε. Our results show that the logarithm of the mean residence time for Gaussian diffusions scales with ε^{-2}, while, instead, a much weaker dependence is found for the Lévy case. Indeed, we find that the mean residence time is proportional to $\varepsilon^{-\alpha}$, where α is the stability parameter of the noise law. This result is in agreement with what has been proven in some special cases for additive Lévy noise, and might indicate that these scaling properties are more general than usually assumed.

Secondly, the results obtained for the most probable transition paths confirm that, in the weak-noise limit, escapes from basins of attraction driven by Gaussian noise take place through the edge state. Additionally, instantonic and relaxation portions within each basin of attraction are clearly distinct, indicating nonequilibrium conditions, yet qualitatively similar. In turn, Lévy diffusions leave the basin through the boundaries region closest to the outgoing attractor, which seems to be the vicinity of the edge state when the thawing transition is considered. The freezing transition, instead, proceeds along a path that is fundamentally different. Finally, the most probable transition paths for the Lévy case appear to depend very weakly on the value of the stability parameter α, but seem, instead, determined by the nature of the Lévy noise of being a jump process.

Our findings provide strong evidence that choosing noise laws other than Gaussian leads to fundamental changes in the metastability properties of a system, both in terms of statistics of the transitions between competing basins of attraction and most probable paths for such transitions. Leaving the door open for general noise laws might be relevant both for interpreting observational data and for performing modelling exercises for the climate system and complex systems in general.

Let's give an example of the impact of making a wrong assumption on the nature of the acting stochastic forcing. Were we to naively interpret one of the panels of Fig. 5 as resulting from the dynamics of a dynamical system perturbed by Gaussian noise, we would have to conclude that the unperturbed deterministic system possesses at least two edge states on the basin boundary separating the competing basins of attraction; see Margazoglou et al. (2021) for a case where this situation applies. Hence, we would infer fundamentally wrong properties on the geometry of the phase space.

https://doi.org/10.5194/npg-2021-34
Preprint. Discussion started: 5 November 2021

Nonlinear Processes in Geophysics
Discussions
Open Access
EGU

We might think of Gaussian noise as being associated to the impact of unresolved scales of motion on the resolved ones or actual random fluctuations of some external parameter. Instead, one might interpret α-stable Lévy noise as describing succinctly, the impact of what in the insurance sector are called acts of God (e.g. an asteroid hitting the Earth; a massive volcanic eruption; the sudden collapse of the West Antarctic ice sheet). Hence, it might be worth investigating the properties of systems where the stochastic forcing comes as the result of simultaneous Gaussian and $\alpha-$stable Lévy noise perturbations.

Data availability. All the data used to produce the figures contained in this paper are publicly available as supplementary material in Lucarini et al. (2021) through the data repository `https://doi.org/10.6084/m9.figshare.16802503`.

Video supplement. Illustrative animations portraying noise-induced transitions can be found in the supplementary material. We further uploaded the relevant material in the `YouTube` platform with links: Lévy SB→W, Lévy W→SB, Gaussian SB→W, Gaussian W→SB.

Author contributions. All authors contributed equally to this work.

Competing interests. One the authors is member of the NPG editorial board. No other competing interests are present

Acknowledgements. The authors wish to thank J. Duan, M. Ghil, T. Grafke, S. Kalliadasis, A. Laio, and G. Pavliotis, for useful exchanges on various topics covered in this paper, and R. Börner for useful remarks in the manuscript. VL wishes to thank M. Allen for suggesting to look into 3D projections of the phase space. The authors acknowledge the support provided by the EU Horizon 2020 project TiPES (grant No. 820970). VL acknowledge the support provided by the EPSRC project EP/T018178/1. This paper is dedicated to K. Hasselmann.

Appendix A: Stochastic perturbations of Lévy type.

In this section we revise the basic properties of a symmetric α-stable Lévy process in a Hilbert space in which the solutions to SPDE (10) are defined. It is pertinent to refer to the distribution law of Lévy increments, its characteristic function, the Lévy-Itô decomposition and the Lévy jump measure for a deeper study of the metastable behavior of the stochastic climate system (10). Let $(\Omega, \mathcal{F}, \mathbb{P})$ be a given complete probability space and $H(\|\cdot\|, \langle\cdot,\cdot\rangle)$ a separable Hilbert space with norm $\|\cdot\|$ and inner product $\langle\cdot,\cdot\rangle$. A stochastic process $(L^\alpha(t)_{t\geq 0})$ is a symmetric α-stable Lévy process in H if it satisfies:

1) $L^\alpha(0) = 0$, a.s..

https://doi.org/10.5194/npg-2021-34
Preprint. Discussion started: 5 November 2021

Nonlinear Processes in Geophysics
Discussions
Open Access
EGU

2) Independent increments: for any $n \in \mathbb{N}$ and $0 \leqslant t_1 < t_2 < \cdots < t_{n-1} < t_n$ the vector

$$(L^\alpha(t_1) - L^\alpha(t_0), \ldots, L^\alpha(t_n) - L^\alpha(t_{n-1})) \tag{A1}$$

is a family of independent random vectors in H.

3) Stationary increments: for $0 \leqslant l < t$ random vectors $L^\alpha(t) - L^\alpha(l)$ and $L^\alpha(t-l)$ have the same law $\mathfrak{L}(.)$ in H

$$\mathfrak{L}(L^\alpha(t) - L^\alpha(l)) = \mathfrak{L}(L^\alpha(t-l)). \tag{A2}$$

4) Sample paths are continuous in probability, i.e. for any $t \geqslant 0$ and $\eta > 0$

$$\lim_{l \to t} \mathbb{P}(\|L^\alpha(t) - L^\alpha(l)\| > \eta) = 0. \tag{A3}$$

Although neither the incremental nor the marginal distribution of a Lévy process in general are representable by the elementary functions, the Lévy motion is completely determined by the Lévy-Khintchine formula which specifies the characteristic function of the Lévy process.

If $L^\alpha(t)$ is a symmetric α-stable Lévy process in H, then:

1) (Lévy-Khintchine formula) Its characteristic function is

$$\Lambda_t(h) = \mathbb{E}\left[e^{i\langle h, L^\alpha(t)\rangle}\right] = e^{t\psi(h)}, \qquad h \in H, \qquad t \geq 0,$$

where

$$\psi(h) = \int_H \left(e^{i\langle h,y\rangle} - 1 - i\langle h,y\rangle \mathbf{1}_{\{0<\|y\|\leqslant 1\}}\right) \nu(dy), \tag{A4}$$

here $\mathbf{1}_S$ is the indicator function for a set S, taking 1 on S and 0 otherwise, and ν is a Borel measure (so called the Lévy jump measure) in H for which $\int_H (1 \wedge \|y\|^2)\nu(dy) < \infty$ with $1 \wedge \|y\|^2 = \min\{1, \|y\|^2\}$. A Borel measure, as well, can be defined as the expected value of the number of jumps of specified size Q in the unit time interval, i.e. $\nu(Q) = \mathbb{E}N(1,Q)(\omega)$, $\omega \in \Omega$.

2) (Lévy-Itô decomposition) For any sequence of positive radii $r_n \to 0$ and $\mathcal{O}_n = \{y \in H \mid r_{n+1} < ||y|| \leqslant r_n\}$ there exist a sequence of independent compensated compound Poisson processes $(\bar{L}_n(t))_{t\geqslant 0}$, $n \geqslant 0$ in H with jump measures $\nu_n(B) = \nu(B \cap \mathcal{O}_n)$ for $B \in \mathcal{B}(H)$ the Borel σ-algebra in H and $n \geqslant 1$, which satisfy $\mathbb{P}$-almost surely for all $t \geqslant 0$

$$L(t) = \sum_{n=1}^{\infty} \bar{L}_n + L_0(t), \tag{A5}$$

$$\bar{L}_n(t) = L_n(t) - t\int_H y\nu_n(dy), \quad n \geqslant 1. \tag{A6}$$

3) Its Lévy jump measure ν is symmetric in the sense that $\nu(-Q) = \nu(Q)$ for $Q \in \mathcal{B}(H)$ and has the specific geometry

$$\nu(Q) = \int_Q \nu(dy) = \int_Q \frac{dr}{r^{1+\alpha}}\sigma(ds), \tag{A7}$$

where $r = \|y\|$ and $s = y/\|y\|$ and $\sigma : \mathcal{B}(\partial B_1(0)) \to [0,\infty)$ is an arbitrary finite Radon measure on the unit sphere of H.

One can come to more intuitive interpretation of the stability parameter $\alpha \in (0,2)$ variation: for smaller values of α, the process is characterized by higher jumps with a lower frequency. As α increases, jumps decrease in height and the frequency of their occurrence increases.

https://doi.org/10.5194/npg-2021-34
Preprint. Discussion started: 5 November 2021

Nonlinear Processes in Geophysics
Discussions
Open Access
EGU

Appendix B: Probabilistic theory for the Lévy noise-induced escape.

We briefly recapitulate here the main ideas behind the proof given in Debussche et al. (2013) of how the mean residence time in the competing metastable states of stochastically perturbed Chafee-Infante reaction-diffusion PDE scales with the intensity ε of the additive $L(t)$ $\alpha-$stable Lévy noise that acts as stochastic forcing.

One proceeds by considering the decomposition of the driving Lévy process with regularly varying jump measure ν into small ξ^ε and large η^ε jump components. Let $\Delta_t L = L(t) - L(t-)$ denote the jump increment of L at time $t \geqslant 0$, and $\frac{1}{\varepsilon^\rho}$ for $\varepsilon, \rho \in (0,1)$ the jump height threshold of L. The process η^ε is a compound Poisson process consisting of all jumps of height $\|\Delta_t L\| > \varepsilon^{-\rho}$ with intensity

$$\beta_\varepsilon = \nu\left(\frac{1}{\varepsilon^\rho} B_1^c(0)\right) \approx \varepsilon^{\alpha\rho}, \tag{B1}$$

and the jump probability measure outside the ball $\frac{1}{\varepsilon^\rho} B_1(0)$ by

$$\nu\left(\cdot \cap \frac{1}{\varepsilon^\rho} B_1^c(0)\right) / \beta_\varepsilon, \tag{B2}$$

where $B_1(0)$ is the ball in H with center in origin and unit radius. The occurrence time of a k-th large jump is defined recursively by

$$\mathcal{Z}_0 = 0, \quad \mathcal{Z}_k = \inf\{t > \mathcal{Z}_{k-1} \mid \|\Delta_t L\| > \varepsilon^{-\rho}\}, \quad k \geqslant 1. \tag{B3}$$

The waiting times between sucessive η_t^ε jumps have an exponential distribution $\mathcal{Z}_k - \mathcal{Z}_{k-1} \sim \mathrm{Exp}(\beta_\varepsilon)$.

Small jump processes $\xi^\varepsilon = L - \eta^\varepsilon$ due to the symmetry of Lévy measure ν is a mean zero martingale in H with finite exponential moments. Probabilistic events causing small jumps in the stochastic solution of the system are not able to overcome the "force" of its deterministic stable state and therefore, do not contribute to the exit from the basin of attraction. Formally, during the time between two large jumps $t_k = \mathcal{Z}_k - \mathcal{Z}_{k-1}$, the solution of (10) following the deterministic path (1) returns to a small vicinity of the stable equilibria $\phi^{W/SB}$

$$\sup_{x \in D^{W/SB}} \sup_{\mathcal{Z}_{k-1} \leqslant t \leqslant \mathcal{Z}_k} \|\mathcal{T}(t) - T(t)\| \to 0 \qquad \text{for} \qquad \varepsilon \to 0. \tag{B4}$$

When a first large jump occurs, the solution process moves to the neighboring domain of attraction with probability

$$\begin{aligned} &\mathbb{P}(\phi^{W/SB} + \varepsilon\Delta_{t_i} L \notin D^{W/SB}) = \mathbb{P}\left(\Delta_{t_i} L \in \frac{1}{\varepsilon}[(D^{W/SB})^c - \phi^{W/SB}]\right) \\ &= \frac{\nu(\frac{1}{\varepsilon}[(D^{W/SB})^c - \phi^{W/SB}] \cap \frac{1}{\varepsilon^\rho} B_1^c(0))}{\nu(\frac{1}{\varepsilon^\rho} B_1^c(0))} \approx \varepsilon^{\alpha(1-\rho)}. \end{aligned} \tag{B5}$$

This is the probability that at time t_i there will be a jump increment $\Delta_{t_i} L$ that exceeds the distance between the attractor and its domain of attraction boundary, expressed by the jump probability measure (B2). In the zero-noise limit the mean residence time in a basin of attraction is given by

https://doi.org/10.5194/npg-2021-34
Preprint. Discussion started: 5 November 2021


Nonlinear Processes in Geophysics
Discussions
Open Access
EGU

$$\mathbb{E}[\tau(\varepsilon)] \approx \sum_{i=1}^{\infty} \mathbb{E}[\mathcal{Z}_i]\, \mathbb{P}[\inf\{j : \phi^{W/SB} + \varepsilon\Delta_{t_j} L \notin D^{W/SB}\} = i]$$
$$\approx \mathbb{E}[t_1]\, \mathbb{P}(\phi^{W/SB} + \varepsilon\Delta_{t_1} L \notin D^{W/SB}) \cdot \sum_{i=1}^{\infty} i\, (1 - \mathbb{P}[\phi^{W/SB} + \varepsilon\Delta_{t_1} L \notin D^{W/SB}])^{i-1}$$
$$\approx \frac{1}{\varepsilon^{\alpha\rho}} \varepsilon^{\alpha(1-\rho)} \left(\frac{1}{\varepsilon^{\alpha(1-\rho)}}\right)^2 = \frac{1}{\varepsilon^{\alpha}}, \tag{B6}$$

i.e. by the sum of all the mean values of large jump occurrence time times the probability that the minimum of a sample of size i of jump increments is sufficiently large to get into the neighboring domain of attraction. Thus, at the random time instant of large jumps, the solution process transitions, in an abrupt move, from one attractor to another. Such behavior of the random dynamical system is known as a metastability.

In Debussche et al. (2013) it was proved that in the time scale $\lambda(\varepsilon) = \nu(\frac{1}{\varepsilon} B_1^c(0))$, $\varepsilon > 0$ the metastable shifting of the diffusion process between neighborhoods of the two attractors represents a continuous time Markov chain in state space $\{\phi^{SB}, \phi^{W}\}$ with a transition rate matrix $\mathfrak{Q}$

$$\mathfrak{Q} = \frac{1}{\mu(B_1^c(0))} \begin{pmatrix} -\mu((D^{SB} - \phi^{SB})^c) & \mu((D^{SB} - \phi^{SB})^c) \\ \mu((D^{W} - \phi^{W})^c) & -\mu((D^{W} - \phi^{W})^c) \end{pmatrix}, \tag{B7}$$

where $\mu(\cdot)$ is the limit measure of ν.

Appendix C: Estimates for the mean residence time

https://doi.org/10.5194/npg-2021-34
Preprint. Discussion started: 5 November 2021

Nonlinear Processes in Geophysics
Discussions
Open Access
EGU

(a)

ε	0.0001	0.0003	0.0005	0.0007	0.0009	0.0011	0.0013	0.0015	0.0017	0.0019
N^o SB $\rightarrow$ W	74	121	162	193	191	218	239	264	286	307
N^o W $\rightarrow$ SB	74	121	162	194	191	218	239	265	287	307
$\mathbb{E}\,[\tau_{SB}]$	715	457	348	290	299	255	218	216	208	178
$CI_{0.95}\,[\tau_{SB}]$	[627,803]	[409,504]	[298,397]	[246,333]	[263,335]	[222,288]	[190,245]	[191,241]	[185,232]	[158,198]
$\mathbb{E}\,[\tau_W]$	618	367	265	226	224	203	200	160	139	146
$CI_{0.95}\,[\tau_W]$	[540,695]	[329,404]	[221,310]	[189,263]	[191,256]	[177,229]	[172,228]	[141,179]	[124,154]	[130,162]

(b)

ε	0.004	0.006	0.01	0.014	0.018	0.022	0.026	0.03	0.034	0.038
N^o SB $\rightarrow$ W	35	50	90	121	152	186	224	255	273	328
N^o W $\rightarrow$ SB	35	51	90	121	152	187	224	256	273	329
$\mathbb{E}\,[\tau_{SB}]$	1461	1029	568	388	344	265	249	202	189	160
$CI_{0.95}\,[\tau_{SB}]$	[1235,1687]	[872,1186]	[482,654]	[336,441]	[306,382]	[230,301]	[216,281]	[178,227]	[166,211]	[143,176]
$\mathbb{E}\,[\tau_W]$	1357	925	531	431	313	270	197	187	177	144
$CI_{0.95}\,[\tau_W]$	[1124,1589]	[782,1067]	[461,600]	[382,481]	[279,347]	[232,307]	[171,223]	[164,211]	[156,197]	[127,161]

(c)

ε	0.01	0.015	0.025	0.035	0.045	0.055	0.065	0.075	0.085	0.095
N^o SB $\rightarrow$ W	5	8	21	37	57	78	118	142	170	231
N^o W $\rightarrow$ SB	5	9	22	37	58	79	118	142	170	231
$\mathbb{E}\,[\tau_{SB}]$	7226	4410	2025	1383	800	629	418	308	282	191
$CI_{0.95}\,[\tau_{SB}]$	[5473,8979]	[3458,5362]	[1526,2525	[1103,1664]	[677,923]	[529,729]	[366,470]	[256,361]	[242,323]	[165,217]
$\mathbb{E}\,[\tau_W]$	9544	6199	2418	1249	904	637	425	395	304	241
$CI_{0.95}\,[\tau_W]$	[7402,11686]	[4772,7625]	[1877,2959]	[1033,1464]	[770,1037]	[546,727]	[363,487]	[329,460]	[259,350]	[207,276]

(d)

ε	0.14	0.16	0.18	0.20	0.22	0.24	0.26	0.28	0.30
N^o SB $\rightarrow$ W	1	9	27	64	109	155	217	269	360
N^o W $\rightarrow$ SB	1	10	27	64	109	156	217	269	359
$\mathbb{E}\,[\tau_{SB}]$	5038	1838	908	394	307	222	187	137	109
$CI_{0.95}\,[\tau_{SB}]$	[2378,7698]	[1138,2538]	[745,1071]	[328,460]	[268,345]	[198,246]	[164,210]	[120,154]	[99, 119]
$\mathbb{E}\,[\tau_W]$	25870	7700	2656	1153	605	418	273	234	168
$CI_{0.95}\,[\tau_W]$	[15339,36401]	[4991,10410]	[2121,3191]	[942,1364]	[524,686]	[377,459]	[238,308]	[208,259]	[151,186]

Table A1. Estimates and 95%-confidence intervals for the mean residence time τ in W and SB basins for Lévy noise with (a) $\alpha = 0.5$, (b) $\alpha = 1.0$, (c) $\alpha = 1.5$, and (d) Gaussian noise. By N^o we calculate the average number of transitions per 10^5 years of temporal evolution.

https://doi.org/10.5194/npg-2021-34
Preprint. Discussion started: 5 November 2021


Nonlinear Processes in Geophysics Discussions
Open Access
EGU

References

Abbot, D. S., Voigt, A., and Koll, D.: The Jormungand global climate state and implications for Neoproterozoic glaciations, Journal of Geophysical Research: Atmospheres, 116, https://doi.org/10.1029/2011JD015927, 2011.

Alharbi, R.: Nonlinear parabolic stochastic partial differential equation with application to finance. Doctoral thesis (PhD), University of Sussex, http://sro.sussex.ac.uk/id/eprint/96730, 2021.

Applebaum, D.: Lévy Processes and Stochastic Calculus, Cambridge Studies in Advanced Mathematics, Cambridge University Press, 2 edn., https://doi.org/10.1017/CBO9780511809781, 2009.

Ashwin, P., Wieczorek, S., Vitolo, R., and Cox, P.: Tipping points in open systems: bifurcation, noise-induced and rate-dependent examples in the climate system, Philosophical Transactions of the Royal Society A: Mathematical, Physical and Engineering Sciences, 370, 1166–1184, https://doi.org/10.1098/rsta.2011.0306, 2012.

Barker, S., Knorr, G., Edwards, R. L., Parrenin, F., Putnam, A. E., Skinner, L. C., Wolff, E., and Ziegler, M.: 800,000 Years of Abrupt Climate Variability, Science, 334, 347–351, https://doi.org/10.1126/science.1203580, 2011.

Benzi, R., Sutera, A., and Vulpiani, A.: The mechanism of stochastic resonance, Journal of Physics A: Mathematical and General, 14, L453–L457, https://doi.org/10.1088/0305-4470/14/11/006, 1981.

Bódai, T., Lucarini, V., Lunkeit, F., and Boschi, R.: Global instability in the Ghil–Sellers model, Climate Dynamics, 44, 3361–3381, 2015.

Bouchet, F., Gawedzki, K., and Nardini, C.: Perturbative calculation of quasi-potential in non-equilibrium diffusions: a mean-field example, Journal of Statistical Physics, 163, 1157–1210, https://doi.org/10.1007/s10955-016-1503-2, 2016.

Brunetti, M., Kasparian, J., and Vérard, C.: Co-existing climate attractors in a coupled aquaplanet, Climate Dynamics, 53, 6293–6308, https://doi.org/10.1007/s00382-019-04926-7, 2019.

Budhiraja, A. and Dupuis, P.: A variational representation for positive functionals of infinite dimensional Brownian motion, Probability and mathematical statistics-Wroclaw University, 20, 39–61, 2000.

Budhiraja, A., Dupuis, P., and Maroulas, V.: Large deviations for infinite dimensional stochastic dynamical systems, The Annals of Probability, 36, 1390 – 1420, https://doi.org/10.1214/07-AOP362, 2008.

Budyko, M. I.: The effect of solar radiation variations on the climate of the Earth, Tellus, 21, 611–619, https://doi.org/10.3402/tellusa.v21i5.10109, 1969.

Burrage, K. and Lythe, G.: Accurate stationary densities with partitioned numerical methods for stochastic partial differential equations, Stochastics and Partial Differential Equations: Analysis and Computations, https://doi.org/10.1007/s40072-014-0032-8, 2014.

Cai, R., Chen, X., Duan, J., Kurths, J., and Li, X.: Lévy noise-induced escape in an excitable system, Journal of Statistical Mechanics: Theory and Experiment, 2017, 063 503, https://doi.org/10.1088/1742-5468/aa727c, 2017.

Chechkin, A., Sliusarenko, O., Metzler, R., and Klafter, J.: Barrier crossing driven by Levy noise: Universality and the Role of Noise Intensity, Physical review. E, Statistical, nonlinear, and soft matter physics, 75, 041 101, https://doi.org/10.1103/PhysRevE.75.041101, 2007.

Cialenco, I., Fasshauer, G. E., and Ye, Q.: Approximation of stochastic partial differential equations by a kernel-based collocation method, in: International Journal of Computer Mathematics, https://doi.org/10.1080/00207160.2012.688111, 2012.

Corral, Á. and González, Á.: Power Law Size Distributions in Geoscience Revisited, https://doi.org/10.1029/2018EA000479, 2019.

Dai, M., Gao, T., Lu, Y., Zheng, Y., and Duan, J.: Detecting the maximum likelihood transition path from data of stochastic dynamical systems, Chaos, https://doi.org/10.1063/5.0012858, 2020.

https://doi.org/10.5194/npg-2021-34
Preprint. Discussion started: 5 November 2021

585 Dakos, V., Scheffer, M., Van Nes, E. H., Brovkin, V., Petoukhov, V., and Held, H.: Slowing down as an early warning signal for abrupt climate change, Proceedings of the National Academy of Sciences of the United States of America, https://doi.org/10.1073/pnas.0802430105, 2008.

Davie, A. M. and Gaines, J. G.: Convergence of numerical schemes for the solution of parabolic stochastic partial differential equations, Mathematics of Computation, https://doi.org/10.1090/s0025-5718-00-01224-2, 2000.

590 Debussche, A., Högele, M., and Imkeller, P.: The dynamics of nonlinear reaction-diffusion equations with small lévy noise, Lecture Notes in Mathematics, https://doi.org/10.1007/978-3-319-00828-8_1, 2013.

Ditlevsen, P. D.: Observation of α-stable noise induced millennial climate changes from an ice-core record, Geophysical Research Letters, 26, 1441–1444, https://doi.org/10.1029/1999GL900252, 1999.

Doering, C. R.: A stochastic partial differential equation with multiplicative noise, Physics Letters A, https://doi.org/10.1016/0375-
595 9601(87)90791-2, 1987.

Duan, J.: An introduction to stochastic dynamics, Cambridge University Press, 2015.

Duan, J. and Wang, W.: Effective Dynamics of Stochastic Partial Differential Equations, Elsevier, https://doi.org/10.1016/C2013-0-15235-X, 2014.

Dybiec, B. and Gudowska-Nowak, E.: Lévy stable noise-induced transitions: stochastic resonance, resonant activation and dynamic hystere-
600 sis, Journal of Statistical Mechanics: Theory and Experiment, 2009, P05 004, https://doi.org/10.1088/1742-5468/2009/05/p05004, 2009.

Feudel, U., Pisarchik, A. N., and Showalter, K.: Multistability and tipping: From mathematics and physics to climate and brain—Minireview and preface to the focus issue, Chaos: An Interdisciplinary Journal of Nonlinear Science, 28, 033 501, https://doi.org/10.1063/1.5027718, 2018.

Freidlin, M. I. and Wentzell, A. D.: Random perturbations of dynamical systems, Springer, New York, 1984.

605 Gao, T., Duan, J., Kan, X., and Cheng, Z.: Dynamical inference for transitions in stochastic systems with α-stable Lévy noise, Journal of Physics A: Mathematical and Theoretical, 49, 294 002, https://doi.org/10.1088/1751-8113/49/29/294002, 2016.

Ghil, M.: Climate stability for a Sellers-type model., Journal of the Atmospheric Sciences, https://doi.org/10.1175/1520-0469(1976)033<0003:CSFAST>2.0.CO;2, 1976.

Ghil, M.: A mathematical theory of climate sensitivity or, How to deal with both anthropogenic forcing and natural variability?, in: Climate
610 Change: Multidecadal and Beyond, edited by P., C. C., M., G., M., L., and M., W. J., pp. 31–51, World Scientific/Imperial College Press, 2015.

Ghil, M. and Childress, S.: Topics in Geophysical Fluid Dynamics: Atmospheric Dynamics, Dynamo Theory, and Climate Dynamics, Springer-Verlag, Berlin, 1987.

Ghil, M. and Lucarini, V.: The physics of climate variability and climate change, Rev. Mod. Phys., 92, 035 002,
615 https://doi.org/10.1103/RevModPhys.92.035002, 2020.

Gottwald, G.: A model for Dansgaard-Oeschger events and millennial-scale abrupt climate change without external forcing, Climate Dynamics, 56, https://doi.org/10.1007/s00382-020-05476-z, 2021.

Gottwald, G. A. and Melbourne, I.: Homogenization for deterministic maps and multiplicative noise, Proceedings of the Royal Society A: Mathematical, Physical and Engineering Sciences, 469, 20130 201, https://doi.org/10.1098/rspa.2013.0201, 2013.

620 Gould, S. J.: Wonderful Life: The Burgess shale and the Nature of History, W.W. Norton, New York, 1989.

Grafke, T. and Vanden-Eijnden, E.: Numerical computation of rare events via large deviation theory, Chaos, https://doi.org/10.1063/1.5084025, 2019.

https://doi.org/10.5194/npg-2021-34
Preprint. Discussion started: 5 November 2021

Grafke, T., Grauer, R., and Schäfer, T.: The instanton method and its numerical implementation in fluid mechanics, Journal of Physics A: Mathematical and Theoretical, https://doi.org/10.1088/1751-8113/48/33/333001, 2015.

Grafke, T., Schäfer, T., and Vanden-Eijnden, E.: Long Term Effects of Small Random Perturbations on Dynamical Systems: Theoretical and Computational Tools, in: Recent Progress and Modern Challenges in Applied Mathematics, Modeling and Computational Science, edited by Melnik, R., Makarov, R., and Belair, J., Fields Institute Communications, pp. 17–55, Springer, New York, NY, https://doi.org/10.1007/978-1-4939-6969-2_2, 2017.

Graham, R.: Macroscopic potentials, bifurcations and noise in dissipative systems, in: Fluctuations and Stochastic Phenomena in Condensed Matter, pp. 1–34, Springer, 1987.

Graham, R., Hamm, A., and Tél, T.: Nonequilibrium potentials for dynamical systems with fractal attractors or repellers, Phys. Rev. Lett., 66, 3089–3092, https://doi.org/10.1103/PhysRevLett.66.3089, 1991.

Grebogi, C., Ott, E., and Yorke, J. A.: Fractal Basin Boundaries, Long-Lived Chaotic Transients, and Unstable-Unstable Pair Bifurcation, Phys. Rev. Lett., 50, 935–938, https://doi.org/10.1103/PhysRevLett.50.935, 1983.

Grigoriu, M. and Samorodnitsky, G.: Dynamic Systems Driven by Poisson/Lévy White Noise, in: IUTAM Symposium on Nonlinear Stochastic Dynamics, edited by Namachchivaya, N. S. and Lin, Y. K., pp. 319–330, Springer Netherlands, Dordrecht, 2003.

Hänggi, P.: Escape from a metastable state, Journal of Statistical Physics, 42, 105–148, 1986.

Hasselmann, K.: Stochastic climate models, Part I. Theory, Tellus, 28, 473–485, 1976.

Hoffman, P. F., Kaufman, A. J., Halverson, G. P., and Schrag, D. P.: A Neoproterozoic Snowball Earth, Science, 281, 1342–1346, https://doi.org/10.1126/science.281.5381.1342, 1998.

Hu, J. and Duan, J.: Onsager-Machlup action functional for stochastic partial differential equations with Levy noise, 2020.

Imkeller, P. and Pavlyukevich, I.: First exit times of SDEs driven by stable L'evy processes, Stochastic Processes and their Applications, 116, 611–642, https://doi.org/https://doi.org/10.1016/j.spa.2005.11.006, 2006a.

Imkeller, P. and Pavlyukevich, I.: Lévy flights: transitions and meta-stability, Journal of Physics A: Mathematical and General, 39, L237–L246, https://doi.org/10.1088/0305-4470/39/15/l01, 2006b.

Imkeller, P. and von Storch, J. S.: Stochastic Climate Models, Birkhauser, Basel, 2001.

Jentzen, A. and Kloeden, P. E.: The numerical approximation of stochastic partial differential equations, Milan Journal of Mathematics, https://doi.org/10.1007/s00032-009-0100-0, 2009.

Kloeden, P. E. and Shott, S.: Linear-implicit strong schemes for itô-galkerin approximations of stochastic PDES, Journal of Applied Mathematics and Stochastic Analysis, https://doi.org/10.1155/S1048953301000053, 2001.

Kramers, H.: Brownian motion in a field of force and the diffusion model of chemical reactions, Physica, 7, 284–304, https://doi.org/https://doi.org/10.1016/S0031-8914(40)90098-2, 1940.

Kraut, S. and Feudel, U.: Multistability, noise, and attractor hopping: The crucial role of chaotic saddles, Phys. Rev. E, 66, 015 207, https://doi.org/10.1103/PhysRevE.66.015207, 2002.

Kuhwald, I. and Pavlyukevich, I.: Stochastic Resonance in Systems Driven by α-Stable Lévy Noise, Procedia Engineering, 144, 1307–1314, https://doi.org/https://doi.org/10.1016/j.proeng.2016.05.129, international Conference on Vibration Problems 2015, 2016.

Lenton, T. M., Held, H., Kriegler, E., Hall, J. W., Lucht, W., Rahmstorf, S., and Schellnhuber, H. J.: Tipping elements in the Earth's climate system, Proceedings of the National Academy of Sciences, 105, 1786–1793, 2008.

Lewis, J. P., Weaver, A. J., and Eby, M.: Snowball versus slushball Earth: Dynamic versus nondynamic sea ice?, Journal of Geophysical Research: Oceans, 112, https://doi.org/10.1029/2006JC004037, 2007.

https://doi.org/10.5194/npg-2021-34
Preprint. Discussion started: 5 November 2021


Nonlinear Processes in Geophysics Discussions
Open Access
EGU

Linsenmeier, M., Pascale, S., and Lucarini, V.: Climate of Earth-like planets with high obliquity and eccentric orbits: Implications for habitability conditions, Planetary and Space Science, 105, 43–59, https://doi.org/https://doi.org/10.1016/j.pss.2014.11.003, 2015.

Løkka, A., Øksendal, B., and Proske, F.: Stochastic partial differential equations driven by lévy space-time white noise, Annals of Applied Probability, https://doi.org/10.1214/105051604000000413, 2004.

Lu, Y. and Duan, J.: Discovering transition phenomena from data of stochastic dynamical systems with Lévy noise, Chaos, https://doi.org/10.1063/5.0004450, 2020.

Lucarini, V. and Bódai, T.: Edge states in the climate system: exploring global instabilities and critical transitions, Nonlinearity, 30, R32–R66, https://doi.org/10.1088/1361-6544/aa6b11, 2017.

Lucarini, V. and Bódai, T.: Transitions across Melancholia States in a Climate Model: Reconciling the Deterministic and Stochastic Points of View, Phys. Rev. Lett., 122, 158 701, https://doi.org/10.1103/PhysRevLett.122.158701, 2019.

Lucarini, V. and Bódai, T.: Global stability properties of the climate: Melancholia states, invariant measures, and phase transitions, Nonlinearity, 33, R59–R92, https://doi.org/10.1088/1361-6544/ab86cc, 2020.

Lucarini, V., Fraedrich, K., and Lunkeit, F.: Thermodynamic analysis of snowball Earth hysteresis experiment: Efficiency, entropy production and irreversibility, Quarterly Journal of the Royal Meteorological Society, 136, 2–11, https://doi.org/10.1002/qj.543, 2010.

Lucarini, V., Pascale, S., Boschi, R., Kirk, E., and Iro, N.: Habitability and Multistability in Earth-like Planets, Astronomische Nachrichten, 334, 576–588, https://doi.org/10.1002/asna.201311903, 2013.

Lucarini, V., Blender, R., Herbert, C., Ragone, F., Pascale, S., and Wouters, J.: Mathematical and physical ideas for climate science, Rev. Geophys., 52, 809–859, https://doi.org/10.1002/2013RG000446, 2014a.

Lucarini, V., Serdukova, L., and Margazoglou, G.: Lévy-noise versus Gaussian-noise-induced Transitions in the Ghil-Sellers Energy Balance Model – Supplementary Material, https://doi.org/10.6084/m9.figshare.16802503, 2021.

Margazoglou, G., Grafke, T., Laio, A., and Lucarini, V.: Dynamical landscape and multistability of a climate model, Proceedings of the Royal Society A: Mathematical, Physical and Engineering Sciences, 477, 20210 019, https://doi.org/10.1098/rspa.2021.0019, 2021.

Nicolis, C.: Stochastic aspects of climatic transitions - response to a periodic forcing, Tellus, 34, 308–308, https://doi.org/10.3402/tellusa.v34i3.10817, 1982.

Ott, E.: Chaos in dynamical systems, Cambridge university press, 2002.

Pavliotis, G. and Stuart, A.: Multiscale methods, Texts in applied mathematics : TAM, Springer, New York, NY, 2008.

Peixoto, J. P. and Oort, A. H.: Physics of Climate, AIP Press, New York, New York, 1992.

Penland, C. and Sardeshmukh, P. D.: Alternative interpretations of power-law distributions found in nature, Chaos: An Interdisciplinary Journal of Nonlinear Science, 22, 023 119, https://doi.org/10.1063/1.4706504, 2012.

Peszat, S. and Zabczyk, J.: Stochastic Partial Differential Equations with Levy Noise, https://doi.org/10.1017/cbo9780511721373, 2007.

Pierrehumbert, R., Abbot, D., Voigt, A., and Koll, D.: Climate of the Neoproterozoic, Annual Review of Earth and Planetary Sciences, 39, 417–460, https://doi.org/10.1146/annurev-earth-040809-152447, 2011.

Ragon, C., Lembo, V., Lucarini, V., Vérard, C., Kasparian, J., and Brunetti, M.: Robustness of competing climatic states, 2021.

Risken, H.: The Fokker-Planck equation, Springer, Berlin, 1996.

Saltzman, B.: Dynamical Paleoclimatology: Generalized Theory of Global Climate Change, Academic Press New York, New York, 2001.

Sellers, W. D.: A global climatic model based on the energy balance of the earth-atmosphere system, Journal of Applied Meteorology, 8, 392–400, 1969.

https://doi.org/10.5194/npg-2021-34
Preprint. Discussion started: 5 November 2021

Serdukova, L., Zheng, Y., Duan, J., and Kurths, J.: Metastability for discontinuous dynamical systems under Lévy noise: Case study on Amazonian Vegetation, Scientific Reports, 7, 9336, https://doi.org/10.1038/s41598-017-07686-8, 2017.

Singla, R. and Parthasarathy, H.: Quantum robots perturbed by Levy processes: Stochastic analysis and simulations, Communications in Nonlinear Science and Numerical Simulation, 83, 105 142, https://doi.org/https://doi.org/10.1016/j.cnsns.2019.105142, 2020.

Skeel, R. D. and Berzins, M.: A Method for the Spatial Discretization of Parabolic Equations in One Space Variable, SIAM Journal on Scientific and Statistical Computing, https://doi.org/10.1137/0911001, 1990.

Skufca, J. D., Yorke, J. A., and Eckhardt, B.: Edge of Chaos in a Parallel Shear Flow, Physical Review Letters, 96, 174 101, https://doi.org/10.1103/PhysRevLett.96.174101, 2006.

Solanki, S. K., Krivova, N. A., and Haigh, J. D.: Solar Irradiance Variability and Climate, Annual Review of Astronomy and Astrophysics, 51, 311–351, https://doi.org/10.1146/annurev-astro-082812-141007, 2013.

Steffen, W., Rockström, J., Richardson, K., Lenton, T. M., Folke, C., Liverman, D., Summerhayes, C. P., Barnosky, A. D., Cornell, S. E., Crucifix, M., Donges, J. F., Fetzer, I., Lade, S. J., Scheffer, M., Winkelmann, R., and Schellnhuber, H. J.: Trajectories of the Earth System in the Anthropocene, Proceedings of the National Academy of Sciences, 115, 8252–8259, https://doi.org/10.1073/pnas.1810141115, 2018.

Thompson, W. F., Kuske, R. A., and Monahan, A. H.: Reduced α-stable dynamics for multiple time scale systems forced with correlated additive and multiplicative Gaussian white noise, Chaos: An Interdisciplinary Journal of Nonlinear Science, 27, 113 105, https://doi.org/10.1063/1.4985675, 2017.

Varadhan, S. R. S., Freidlin, M. I., and Wentzell, A. D.: Random Perturbations of Dynamical Systems., Journal of the American Statistical Association, https://doi.org/10.2307/2287939, 1985.

Voigt, A. and Marotzke, J.: The transition from the present-day climate to a modern Snowball Earth, Climate Dynamics, 35, 887–905, https://doi.org/10.1007/s00382-009-0633-5, 2010.

Vollmer, J., Schneider, T. M., and Eckhardt, B.: Basin boundary, edge of chaos and edge state in a two-dimensional model, New Journal of Physics, 11, 013 040, https://doi.org/10.1088/1367-2630/11/1/013040, 2009.

Weron, A. and Weron, R.: Computer simulation of Levy alpha-stable variables and processes, Chaos: The Interplay Between Stochastic and Deterministic Behaviour, 1995.

Wu, J., Xu, Y., and Ma, J.: Lévy noise improves the electrical activity in a neuron under electromagnetic radiation, PloS one, 12, e0174 330–e0174 330, https://doi.org/10.1371/journal.pone.0174330, 2017.

Yagi, A.: Abstract Parabolic Evolution Equations and their Applications, Springer Monographs in Mathematics, Springer Berlin Heidelberg, https://books.google.co.uk/books?id=zBjYhyp4634C, 2009.

Zheng, Y., Serdukova, L., Duan, J., and Kurths, J.: Transitions in a genetic transcriptional regulatory system under Lévy motion, Scientific Reports, 6, 29 274, https://doi.org/10.1038/srep29274, 2016.

Zheng, Y., Yang, F., Duan, J., Sun, X., Fu, L., and Kurths, J.: The maximum likelihood climate change for global warming under the influence of greenhouse effect and Lévy noise, Chaos, https://doi.org/10.1063/1.5129003, 2020.